Inflammation of the Central Nervous System

– Modeling Multiple Sclerosis as a Motile Excitable Medium

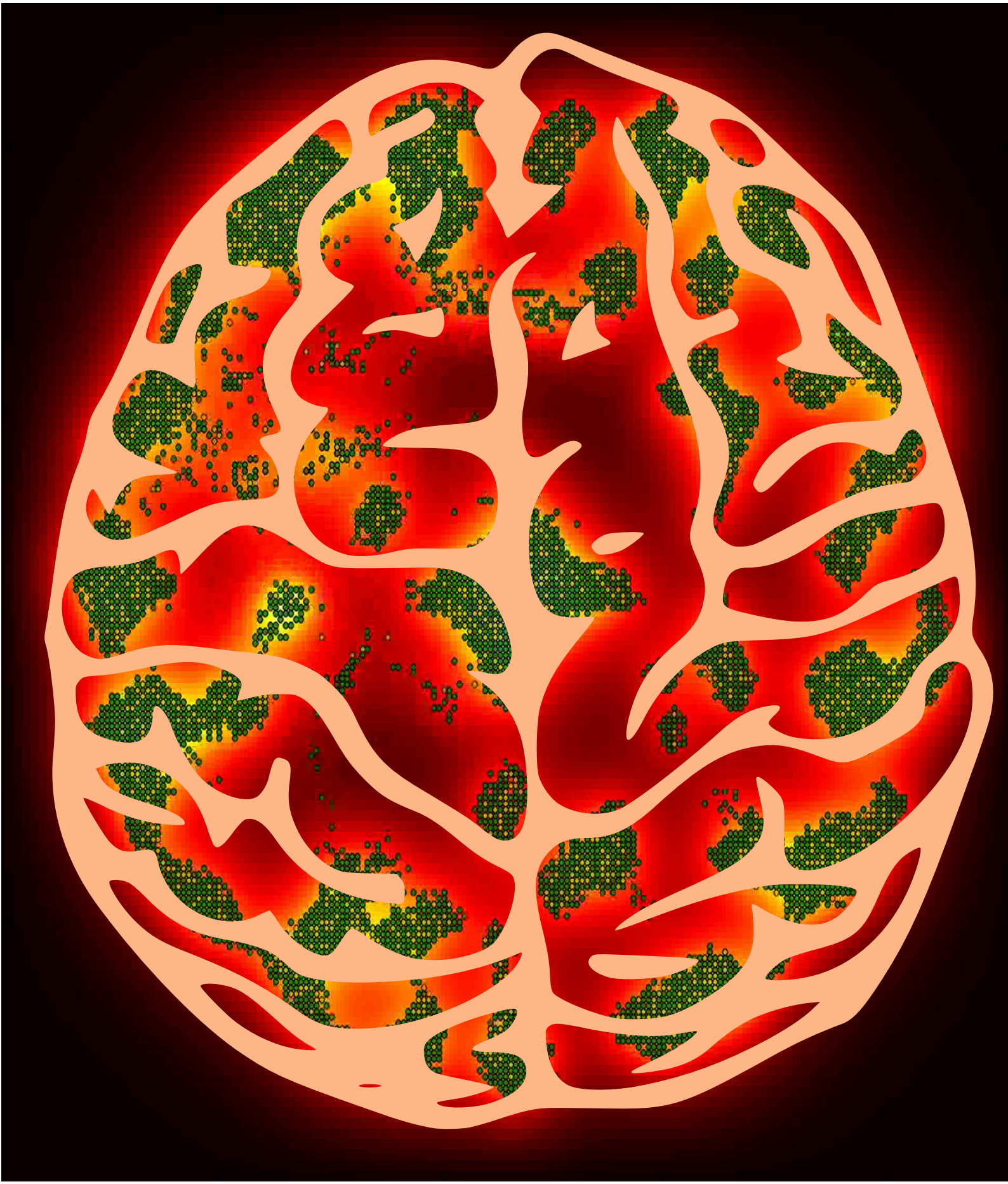

Rógvi Dávid Arge

FACULTY OF SCIENCE
UNIVERSITY OF COPENHAGEN

Inflammation of the Central Nervous System

Modeling Multiple Sclerosis as Motile Excitable Medium

Rógvi Dávid Arge

Academic Supervisor's:
Mogens Høgh Jensen & Ala Trusina

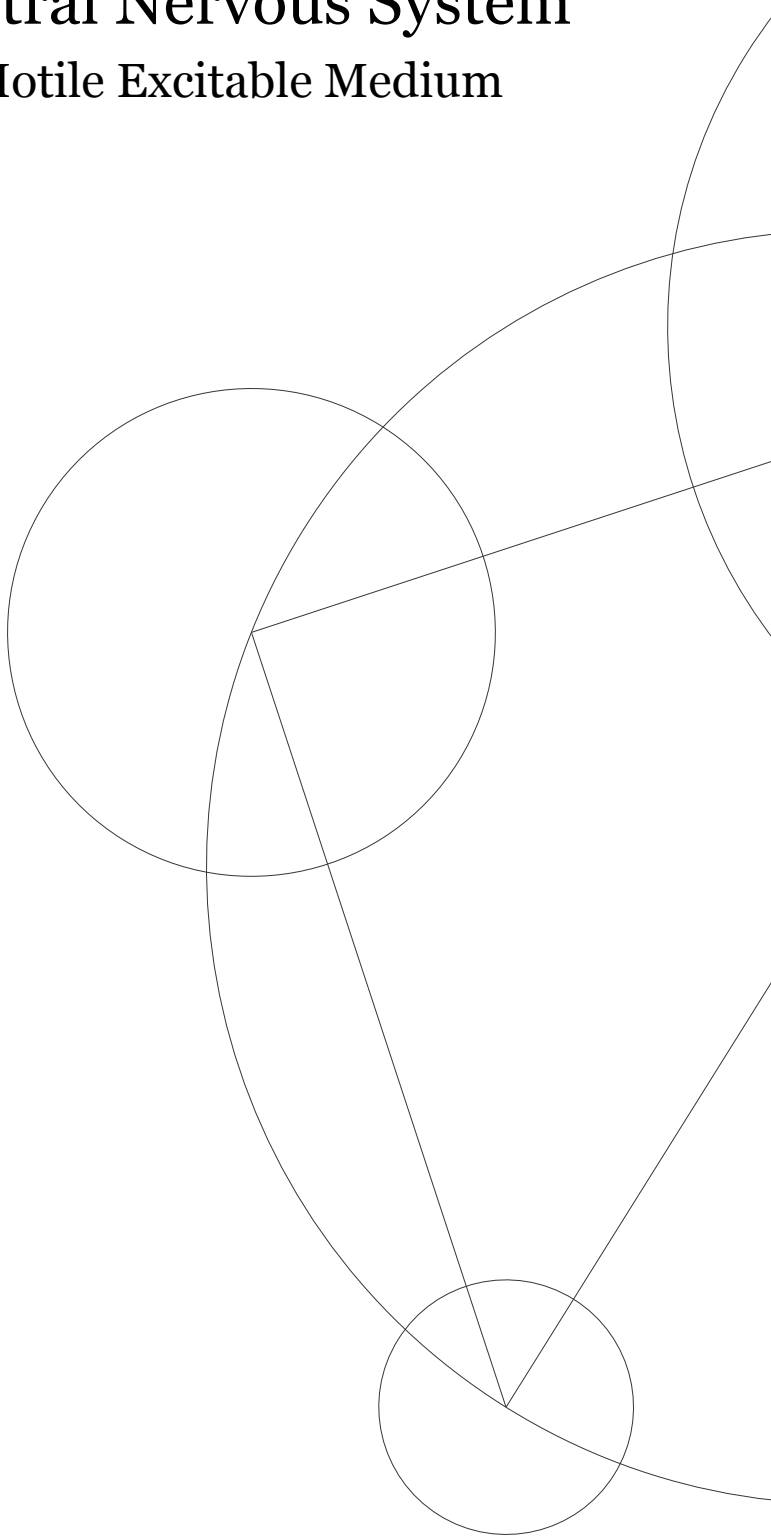

A thesis presented for the degree of
Master of Science in Physics

Niels Bohr Institute
Copenhagen University
Submitted: 22. April, 2015

Abstract

The pro-inflammatory cytokines IFN-γ, TNF-α and IL-1β are an essential part of macrophage polarization and of the inflammatory response in macrophages. Macrophages remove cellular debris, foreign substances and microbes in a process called phagocytosis, and are a vital part of the immune system. However, for various unknown reasons, the inflammatory response can get activated by substances and tissue normally present in the body, which in many cases leads to chronic inflammation. This is the case in multiple sclerosis (MS), a so called autoimmune disease, in which macrophages remove the isolating myelin-layer from axons in the central nervous system (CNS), resulting in plaques. But different types of MS result in different plaque patterns, as well as different sizes of the plaques. In this thesis using a mathematical model I wish to address the questions: What limits plaque size in MS? Under which circumstances is plaque formation possible? And how is inflammation resolved?

In this thesis I focus on pro-inflammatory macrophages, the activation of NF-κB, and the chemotactic movement of macrophages. I therefore neglect T-cells, the recruitment and polarization of M1 macrophages, as well as anti-inflammatory M2 macrophages and their effects. These assumptions simplify the complex processes of the inflammatory response, resulting in a simpler model for inflammation in macrophages. I apply and modify a model previously developed for the inflammatory response in neutrophils to fit a system of macrophages. Furthermore, I introduce macrophage motility. The model has two free parameters p and S, where p is a cytokine production rate, and S is a basal cytokine production level. A mathematical analysis of the model shows that a single macrophage is bistable given that p exceeds a threshold level.

Based on simulations I show that macrophages can accumulate into plaques, and that the number of plaques and their size depends on the diffusion constant, the parameter p, and the number of macrophages. I find a linear relation between the diffusion constant and the average plaque size, when p is low, as well as a linear relation between the average plaque size and the number of macrophages, when p is high. Furthermore I show that there is a qualitative differences between a low p system and a high p system. Inspired by the study by [Starossom et al., 2012] which shows that plaques can be resolved by introducing GAL1, an inhibitor of the NF-κB activation, I also show possible ways one could resolve plaques through NF-κB activator inhibition or cytokine inhibition.

Resumé

De pro-inflammatoriske cytokiner IFN-γ, TNF-α og IL-1β er en essentiel del af makrofag-polarisering og af den inflammatoriske respons i makrofager. Makrofager fjerner cellerester, fremmede stoffer og mikrober igennem en proces kaldet fagocytose, og er en vital del af immunforsvaret. Men af forskellige ukendte årsager kan det inflammatoriske respons blive aktiveret af stoffer og væv some normalt findes i kroppen. Dette er tilfældet i multipel sklerose (MS), en såkaldt autoimmun sygdomme, som er rettet mod centralnervesystemet (CNS) og hvor makrofager fjerner det isolerende myelin-lag fra axonerne, og hvor resultatet er formationen af plaques. Men forskellige typer af MS resulterer i forskellige plaque mønstre, og forskellige størrelser af plaques. I denne afhandling vil jeg ved brug af en matematisk model prøve at finde svar på spørgsmål som: Hvad afgrænser plaque størrelse i MS? Under hvilke omstændigheder er formationen af plaques mulig? Og hvordan opløses plaques?

I denne afhandling fokuserer jeg på de pro-inflammatoriske makrofager, aktiveringen af NF-κB, og makrofagers kemotaktiske bevægelse. Jeg negligerer derfor T-celler, rekruteringen og polariseringen af M1 makrofager, samt de anti-inflammatoriske M2 makrofager og deres effekt. Disse antagelser simplificerer de komplekse processer som udgør det inflammatoriske respons. Dette resulterer i en simplere model for inflammation i makrofager. Jeg anvender og modificerer en tidligere model, udviklet til det inflammatoriske respons i neutrofiler, til at passe til et system af makrofager. Derudover tilføjer jeg makrofagerne motilitet. Modellen har to frie parametre p og S, hvor p er en cytokin produktions rate og S er en basal cytokin produktion. En matematisk analyse af modellen viser at en enkelt makrofag er bistabil givet at p er over en grænseværdi. Baseret på simuleringer viser jeg at makrofager kan samle sig i plaques, og at antallet af plaques og deres størrelse afhænger af diffusions konstanten, parameteren p, og antallet af makrofager. Jeg finder en lineær relation mellem diffusions konstanten og den gennemsnitlige plaque størrelse, når p er lav, og mellem den gennemsnitlige plaque størrelse og antallet af makrofager, når p er høj. Derudover viser jeg at der er en kvalitativ forskel på et system med lav p og et system med høj p. Inspireret af undersøgelsen af [Starossom et al., 2012], som viser at plaques kan opløses ved at introducere GAL1, en inhibitor af NF-κB aktiveringen, viser jeg også mulige måder at opløse plaques på gennem NF-κB aktivator inhibering eller cytokin inhibering.

Acknowledgements

For the past 12 months I have had the pleasure of writing my master's thesis in the biocomplexity group Center for Models of Life (CMOL). My time here has now come to an end and I would very much like to thank everyone at CMOL for making this year so memorable.

Primary thanks go to my supervisor Mogens Høgh Jensen for discussions and for always being open to ideas. His enthusiasm about the project really lifted me up when I was having doubts. My co-supervisor Ala Trusina who always helped me keep an overview of the project and guided me when I was focusing too much on some small details. The project was her idea and I can't thank her enough for giving me the opportunity to write my master's thesis with her and Mogens. Talking with her always made the most difficult problem seem so simple and she always had a contagiously positive way of looking at things.

A very special thanks goes to Thomas Holst-Hansen for always being willing to help. He showed great interest in the project from day one, and helped me almost daily with everything from mathematical problems to understanding the biological processes of a bistable system. When Mogens was on conferences or giving lectures either here at NBI or in other parts of the world, and Ala was on maternity leave Thomas was the one I went to when facing problems or had any questions. I would also like to thank him for giving me ideas on what to include and not to include in the thesis. If not for him this thesis wouldn't have seen the light of day.

Last but not least I would like to thank my girlfriend Jórun for being so supportive during these past 12 months, where I really wasn't all to available, my friends, who helped me relax when there was time for that, and my family for always asking about the project, giving me ample opportunity to explain in laymans terms what the purpose of the project was.

List of Figures

Contents

1

Introduction

"Make things as simple as possible, but not simpler"
– Albert Einstein

Autoimmune diseases occur when the body's immune system is no longer able to distinguish between healthy tissue and antigens. The result is that the immune system starts targeting healthy tissue, triggering an inflammatory response. This can result in a never ending battle between the immune system trying to both destroy and repair the tissue, and in many cases the result is fatal. Autoimmune diseases are estimated to be among the leading causes of death among women in all age groups up to 65 years. Of the autoimmune diseases that target the central nervous system (CNS), multiple sclerosis (MS) is the most common. In MS, the immune system targets myelin and oligodendrocytes resulting in scarred areas of the brain called plaques. As of 2008 it was estimated that between 2 and 2.5 million people, were affected by this disease, that the disease is more prevalent in colder countries, and that the ratio between women and men with MS is 2:1[World Health Organization et al., 2008]. To date the pathogenesis of MS is unknown, however, it has been shown that both environment and genetics play a big role[Compston and Coles, 2008]. Knowledge of the processes at work in MS are therefore very interesting and any model giving insight into the mechanics of the disease may aid in the understanding and development of better treatment methods.

Myelin
Myelin is a material consisting of $75 - 80\%$ lipids and covers areas of the axons and who's main function is to increase propagation speeds of neural signals

Oligodendrocytes
Oligodendrocytes are a type of neuroglia, which main function is to provide insulation in the form of myelin to axons in the CNS

Modeling of the regulatory network of NF-κB has been done previously [Holst-Hansen; Jensen and Krishna, 2012; Yde et al., 2011a,b,b], but none of them have looked at the behavior of a motile excitable media and its application to disease modeling. Therefore, combining previous work with knowledge of the inflammatory response in MS, a model – incorporating

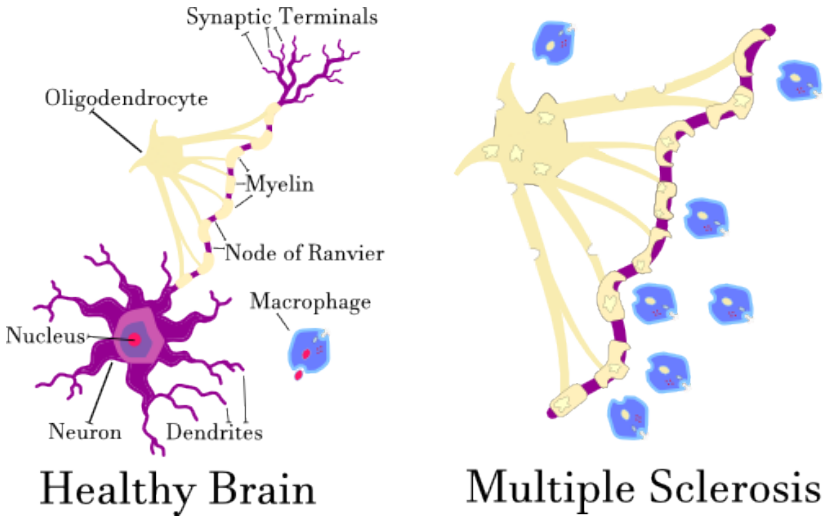

Figure 1.1: Macrophages removing the isolating myelin-layer from the axons and killing the myelin-producing oligodendrocytes.

the bistable nature of inflammatory cells – will be applied to a system of macrophages. The macrophages will be modeled as cellular automatons on a quadratic two dimensional grid and the intracellular NF-κB regulatory network will be modeled by a set of three coupled differential equations. The system is analyzed as a motile excitable medium, where neighboring cells are coupled through diffusion. Parameter settings will be adjusted to model phenomenological observations of plaque (scar-like area of the CNS consisting demyelinated neurons) sizes, diffusion, and macrophage motility in both healthy and inflamed tissue[1].

In MS, macrophages, T-cells and a multitude of other cells are recruited to the lesion site. When macrophages aggregate the extracellular environment will have an effect on how they react. In early stages of MS macrophage reaction will be pro-inflammatory and they start demyelinating the neurons and the oligodendrocytes[2]. With time this results in gliosis, which is the development of glial scar tissue that is nonresponsive to remyelination. This glial scar is called a plaque, and they are usually limited in size[3]. This leads to the first question this study sets out to

[1]Many of the physiological values found in articles regarding MS, like macrophage movement speed, diffusion constant of various cytokines, and production rate of cytokines have been found through in vitro experiments because the technical tools for measurements of these values in the CNS currently aren't good enough or haven't been developed. Given this knowledge, many of the simulations will be run from a lower to an upper bound, for some of the most important parameters in the system.

[2]This is a very simplified explanation of a very complex process. A more detailed explanation of this process is given in Chapter 2

[3]In fulminant multiple sclerosis, which is a borderline form of MS, one develops a large lession that with time can extend to the entirety of the brain[Dimitri P. Agamanolis, 2014]

answer: **what limits plaques from growing infinitely?** This will be answered by simulations to show that the inflammatory process produces a macrophage free zone effectively isolating the inflammation from attracting more macrophages. The second question, which can be thought of as a follow-up to the first one, is: **why do macrophages that have gathered stay in this plaque, and what does it take to dissolve them?**. This will be analyzed with simulations, to show that the most efficient way to dissolve plaques is to inhibit the NF-κB activation by lowering k_{IN}. The study will also show that plaque size is proportional to the diffusion constant D and p, and the number of macrophages.

This study will start with an introduction to the central nervous system and how it is affected by MS. Possible disease pathways will be explored, and macrophages, one of the mediators of inflammation in MS, will be thoroughly explained. The role of NF-κB in the inflammatory process in macrophages will be explained along with the some of the pro-inflammatory cytokines and their role in the regulatory network that perpetuates inflammation. Having described the biological processes and framework, a previously published model will be applied to a system of motile macrophages. Using the model, I will look at the effects of low and high diffusion, p, and number of macrophages, as well as investigate the stability of plaques under various conditions, and excitability of the system under various initial conditions. The results of the simulations and their implications will be discussed and the study will end with a conclusion and outlook.

2

Central Nervous System and Multiple Sclerosis

"Any fool can know. The point is to understand."
– Albert Einstein

Multiple Sclerosis is a demyelinating disease that affects the CNS. Knowledge of the CNS, and the effectors of MS is therefore vital in understanding how a mathematical and computational model can be applied to this system. This chapter will start with an introduction to the CNS and its main functions, and how MS and the inflammatory process affects it. A brief overview over the disease and its progression patterns will be given, and some hypothesis on the pathogenesis of MS will be introduced. The chapter will end with macrophages' role in MS, and their activation process, as these are a central part of the model.

2.1 The Central Nervous System

The central nervous system is the part of the nervous system consisting of the brain and the upper spinal cord, extending from the base of the skull to the first lumbar verterbra figure 2.1. The main function of the spinal cord is the transmission of neural signal between the brain and the body. Most notably the CNS has a complex network of neurons, consisting of on average 86 billion neurons [Azevedo et al., 2009; Herculano-Houzel, 2009] each connected to several thousand other neurons by synapses.

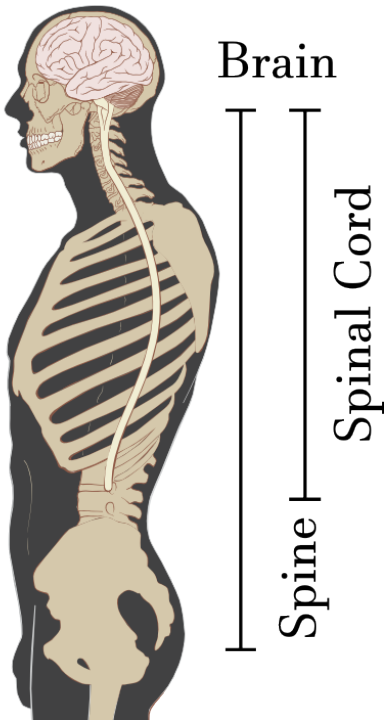

Figure 2.1: Central Nervous System. By Patrick J. Lynch, medical illustrator (Patrick J. Lynch, medical illustrator) [CC BY 2.5 (`http://creativecommons.org/licenses/by/2.5`)], via Wikimedia Commons. Author modified two original illustrations and added text.

The most important function of the CNS w.r.t. this study is the transmission of signals from one region of the brain to another region in either the brain or body. The transmission of signals is done by neurons through neruonal signalling, where the neurons produce an electrical signal that is transmitted via synapses. In some diseases, specifically demyelinating diseases, the transmission of signal is slowed by the removal of myelin from the neurons, whose function is to improve propagation speed of the signal. This is done through a process called saltatory conduction, where the signal "hops" from one node of Ranvier to another increasing the propagation speed from 2 m/s to 200 m/s. The removal of myelin from the neurons therefore has a huge effect on how signal is transmitted, and the severity of demyelinating diseases range from mild, person doesn't know he has the demyelinating disease, to severe, person has impaired muscle coordination, blurred vision etc., to lethal, the person dies. Demyelinating diseases are caused by autoimmune responses, infections, genetics and some by unknown factors. The most common of the demyelinating autoimmune disease which affect the CNS is multiple sclerosis [World Health Organization et al., 2008].

2.2 Multiple Sclerosis

Multiple sclerosis, also known as encephalomyelitis disseminata[1] (encephalo - term for diseases affecting the brain; myelitis - term for diseases affecting the spinal cord) is the most common autoimmune disease affecting the central nervous system. It is a demyelinating autoimmune disease that, due to the randomely attacked locations, has a wide range of signs and symptoms, including physical, mental and psychiatric problems. However, MS is accepted to take on several forms, which are differentiable by the duration, aggresivity and relapse time of the demyelinating attacks. Four patterns of progression,

- Relapsing-remitting (RRMS),
- Secondary-progressive (SPMS),
- Primary-progressive (PPMS),
- Progressive-relapsing (PRMS),

were described by the National Multiple Sclerosis Society in 1966 [Lublin et al., 1996] and have subsequently been used for diagnosing and treating patients. There are other types of MS that have been described, but the debate on whether these really are variants of MS or if they are entirely different diseases is still ongoing [Poser and Brinar, 2007; Wingerchuk and Lucchinetti, 2007].

The pathogenesis of MS is still unknown, but geographic locations and genetics have been shown to be correlated to the frequency of MS cases [Compston and Coles, 2008]. A widely accepted hypothesis, is that a dialogue between T-cell receptors (TCR) on CD4+ T-lymphocytes with myelin antigens presented by class II major histocompatibility complex (MHC) expressed on macrophages/microglia, leads to an immune attack on the myelin-oligodendrocyte complex and an interruption of the blood brain barrier (BBB): *"Exposure of endothelium to pro-inflammatory cytokines (IFN-γ, TNF-α and IL-1β) interrupts the BBB by disorganizing cell-cell junctions, decreases the brain solute barrier, enhances leukocyte endothelial adhesion and migration as well as increases expression of class II MHC and promotes shedding of endothelial 'microparticles' (EMP)."* [Minagar and Alexander, 2003]. Another hypothesis, is that MS is caused by an infectious and viral agent. No clear association with any particular viral pathogen has been found, but some, including human herpevirus 6 (HHV-6)

[1] According to a review article from 2007, MS and DEM are two distinct diseases [Poser and Brinar, 2007]

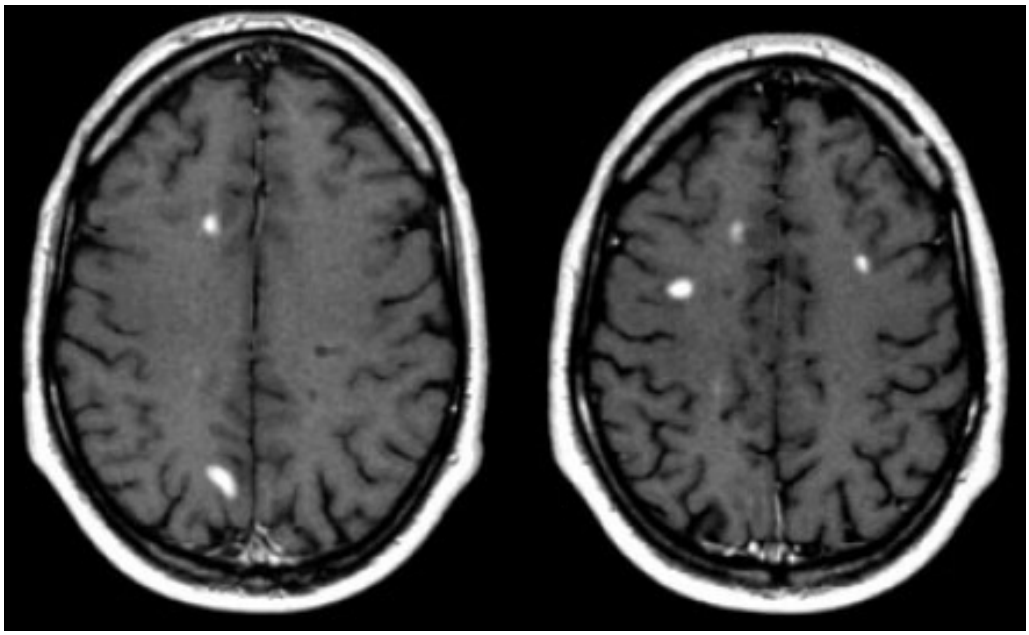

Figure 2.2: T1WI: Multiple enhancing lesions. Retrieved 19, February, 2015, from `http://www.radiologyassistant.nl/en/p4556dea65db62/multiple-sclerosis.html`

T2W
T2-weighted images are MRI images where a spin-spin relaxation has been introduced. Simply put a T2-weighted image is created by allowing magnetization to decay before measuring the MR signal.

FA-maps
Fractional anisotropy is a measure one can compute from the diffusion tensor, which is computed from vector algorithms on a diffusion tensor image.

EDSS
The EDSS goes from 0.0 to 10.0 with 0.0 being normal neurological exam, 1 being no disability, and minimal signs on one Functional System, and 10.0 being death due to MS.

have been implicated on basis of the presence of HHV-6 DNA and antibodies in the blood and cerebral spinal fluid (CSF) of MS patients [Brogden and Guthmiller, 2002; Gilden et al., 2007]. However, HHV-6 is only found in a minority of MS patients, and elevated levels of HHV-6 DNA and antibodies are also seen in patients with other neurological diseases [Gilden et al., 2007].

RRMS, present in $> 80\%$ MS patients, is characterized by the onset of attacks, followed by periods of varying length of remission. In the attacks, myelin is removed from the neurons, some times resulting in astroglial scars called plaques. This is not always the immediate case though and MS lesions sometimes recover to full function before another attack. The plaques are usually multiple with an average plaque size of $72 \pm 21\,\mathrm{mm}^2$ using T2W imaging and $91 \pm 35\,\mathrm{mm}^2$ using FA-maps [Kealey et al., 2005]. They are randomly distributed and have a predilection for the periventricular white matter, optic nerves, and spinal cord but spare no part of the CNS [Brownell and Hughes, 1962]. They may involve gray matter such as cerebral cortex, deep nuclei, and brainstem. In these locations, they involve myelinated axons while sparing the neuronal bodies [Agamanolis].

Though no cure has yet been developed for MS, ongoing trials are researching the possibility of curing it with hematopoietic stem cell transplantation [Burt et al., 2015; Nash et al., 2014]. The results so far have

been promising and patients have an improvement in extended disability state scale (EDSS) score ≥ 1, with a mean EDSS of about 4 at the start of the trial and about 3.1 after 5 years[Burt et al., 2015]. Other approaches to MS treatment include reducing T-and B-cell activation, proliferation, and function in response to autoantigens [O'Connor et al., 2011], induction of antigen-specific tolerance through myelin peptide skin patches[Walczak et al., 2013], and inhibition of pro-inflammatory cytokines through anti-cytokine antibodies [Ruuls and Sedgwick, 1998], all with varying degree of succes.

2.2.1 MS & Inflammation

After the onset of MS and before the first signs of disease become visible, a set of complex processes interact to start the inflammatory process. The simplest way it can be explained, whilst still informing about the processes vital to the development of the model is this: **(1)** TCRs on CD4+ T-lymphocytes interact with myelin antigens presented by class II MHC expressed on monocytes (macrophages/microglia), **(2)** T-lymphocytes start secreting cytokines – most notably interleukin-2 (IL-2) and interferon-γ (IFN-γ) – and chemokines (a family of small cytokines, whose name derives from their ability to induce directed chemotaxis[Groves and Jiang, 1995]). This resutls in a chemotactic response from monocytes, and a pro-inflammatory polarization of macrophages, as well as an interruption of the BBB, **(3)** recruited pro-inflammatory monocytes and toxic cytokines start degrading myelin and oligodendrocytes, **(4)** demyelination and degradation of myelin and oligodendrocytes activates the recruitment of reactive astrocytes, which are capable of recruiting both T_h1 and T_h2 (an anti-inflammatory differentiation of the naïve T helper cell) cells through the secretion of IL-12 and IL-4 respectively, **(5)** pro- and anti-inflammatory monocytes and T-lymphocytes get recruited, differentiating into a phenotype decided by the cytokine environment, **(6)** reactive astrocytes react to the degradation of myelin and neurons by isolating the neurons, resulting in astrogliosis that may, if severe enough, result in inhibition of remyelination and neuronal regrowth.

TCR
The TCR or T cell receptor is a heterodimer found on the surface of T-lymphocytes, and is responsible for recognizing antigens presented by the major histocompatibility complex (MHC) molecules.

MHC class II
Major histocompatibility complex class II molecules are a central part of the antigen presentation process of macrophages. They are loaded by the macrophages through the process of phagocytosis.

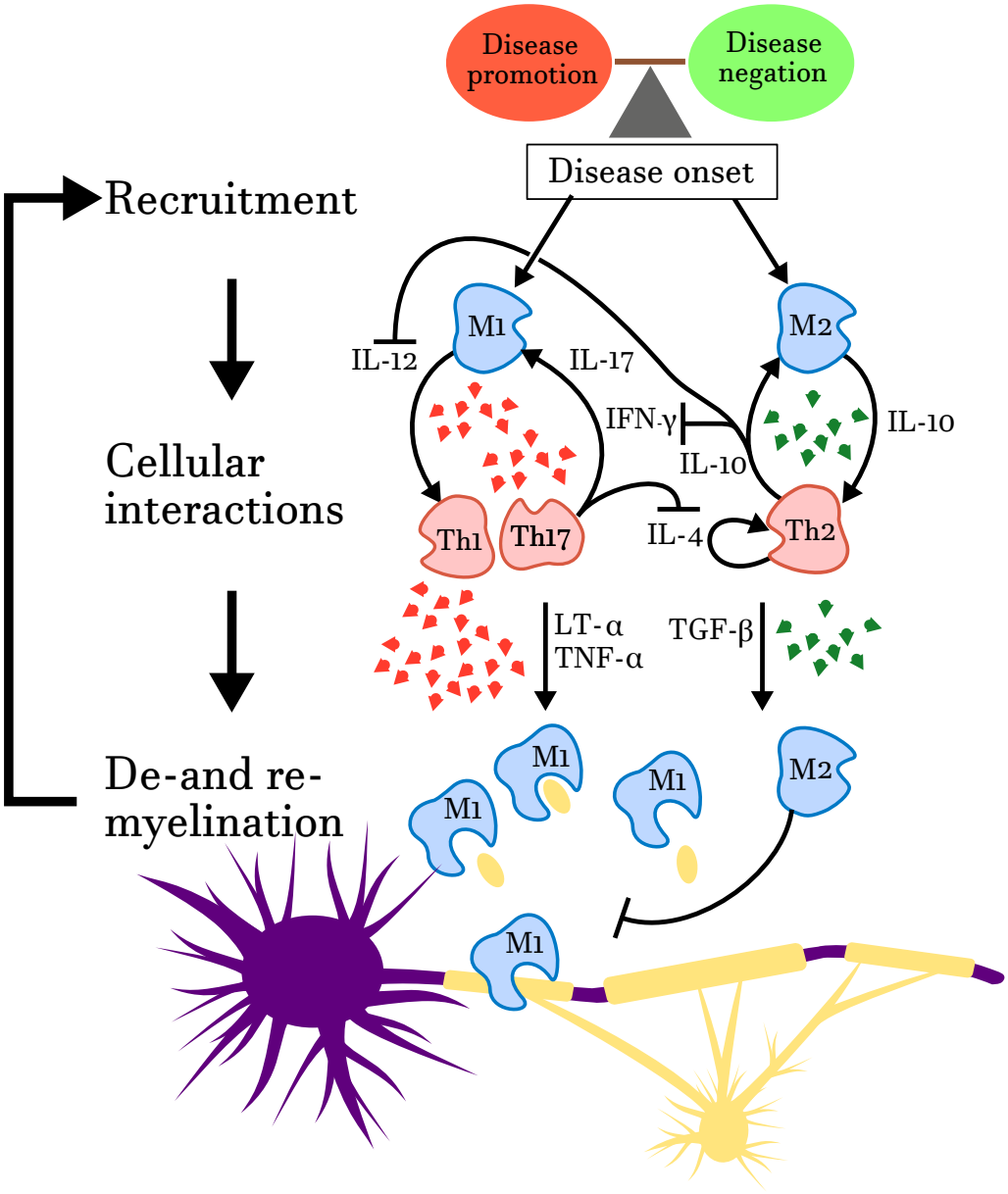

Figure 2.3: Simplified disease development scheme.

The interaction network this study sets out to analyze is a simplified version of the recruitment and cellular interactions seen in figure 2.3 focusing on the aggragation and interactions of macrophages.

2.2.2 Role of Macrophages in MS

Macrophages, and microglia are phagocytes responsible for ingesting (phagocytosing) harmful foreign particles, bacteria, and dead or dying cells. Generally speaking, the two are genetically distinct myeloid populations. Macrophages,

being derived from hematopoietic stem cells in the bone marrow, circulate the peripheral vasculature, and are $30-80\%$ of the phagocyte population in advanced active plaques with partial or complete myelin loss[Li et al., 1996]. Microglia (resident macrophages of the brain) originate from erythromyeloid precursors in the embryonic yolk sac and are 60% of the phagocyte population in early active MS plaques[Ginhoux et al., 2010; Kierdorf et al., 2013; Li et al., 1996]. In inflammation, they have dual roles, being both pro-and anti-inflammatory or immunoregulatory, depending on the differentiation into either M1 (pro-inflammatory) or M2 (anti-inflammatory/immunoregulatory) macrophages, where M1/M2 was chosen to follow the T_h1/T_h2 nomenclature [Martinez and Gordon, 2014]. The exposure to IFN-γ drives M1 polarization [Martinez et al., 2009], inducing a cytotoxic and antitumoral environment, while the exposure to IL-4 drives M2 polarization [Stein et al., 1992], inducing an immunoregulatory environment. Though the M1 phenotype is known to be pro-inflammatory, myelin laden macrophage, also known as a foam cells, have an intermediate activation status Vogel et al. [2013], expressing both M1 and M2 markers, or are actually anti-inflammatory Boven et al. [2006] depending on the source.

Benefits of Macrophages/Microglia in MS

Macrophages, in addition to recruiting reactivating T cells, have been shown to promote the survival of neurons, functional recovery and nerve regeneration[Rapalino et al., 1998]. Macrophages/microglia are also responsible for the removal of myelin debris and reparation of lesions, and studies decreasing microglial activity were shown to actually increase demyelination, delay remyelination and impair oligodendrocyte precursor cell proliferation[Skripuletz et al., 2013].

Macrophages
Macrophages are reported to have a lifespan ranging from days to weeks [Weischenfeldt and Porse, 2008], a diameter of $21\,\mu$m [Krombach et al., 1997] and a movement speed ranging from $10.8\,\mu$m/h [Vereyken et al., 2011] to $600\,\mu$m/h [Pixley, 2012] depending on source and location.

Detrimental effects of Macrophages/Microglia in MS

On the other hand macrophages/microglia have also been observed to strip myelin, as well as kill neurons and oligodendrocyte progenitor cells (OPCs) [Merrill and Zimmerman, 1991; Peterson et al., 2002; Takeuchi et al., 2005]. When macrophages/microglia are activated, they release an array of inflammatory cytokines, such as TNF-α and IFN-γ. These cytokines induce the release of glutamate. Excessive glutamate stimulation on N-methyl-D-aspartate (NMDA) receptors results in mitochondrial death and ultimately excitotoxic neuronal and oligodendrocyte death [Takeuchi et al., 2005]. When glutamate release is blocked, EAE progression is attenuated, providing evidence for glutamate excitotoxicity as a plausible mechanism for macrophage/microglia-mediated toxicity [Shijie et al., 2009]. In addi-

tion to stimulating the release of glutamate, pro-inflammatory cytokines and chemokines promote inflammation and antigen presentation, thereby mediating the recruitment and reactivation of T cells to the lesion [Bauer et al., 1995]. Finally, the release of free radicals, such as nitric oxide (NO), has been shown to induce oxidative damage to neurons and oligodendrocyte precursor cells [Reynolds et al., 2007].[Rawji and Yong, 2013]

2.2.3 The NF-κB Activation Process

The activation of M1 macrophages, induces an auto-regulatory feedback loop, where the nuclear factor kappa-light-chain-enhancer of activated B cells, otherwise known as NF-κB is a central part. NF-κB is a protein complex that controls transcription of DNA and is found in almost all mammalian cells. NF-κB has an active an a passive state, and is said to be passive when it is bound to the inhibitor IκB (inhibitor of κB). Active NF-κB is free to move into the nucleus and turn on the expression of specific genes. NF-κB is activated by many different stimuli, including cytokines, activators of protein kinase C (PKC), viruses and oxidants and acts as a central regulator of the innate and adaptive immune response, cell proliferation and apoptosis[Epstein et al., 1997; Satoh et al., 2007]. There are currently over 150 target genes for NF-κB identified [Pahl, 1999; Satoh et al., 2007]. A significant subset of these, including inflammatory cytokines TNF-α and IL-1β, activate the expression of NF-κB. Though NF-κB is self-activating it also induces the transcription of A20, an inhibitor of the IκB Kinase (IKK) – an enzyme complex that through phosphorylation of the IκBα protein, upregulates NF-κB. Furthermore active NF-κB also turns on the expression of its own repressor IκBα, which binds to NF-κB terminating the transcription resulting in an auto-regulatory loop that amplifies and perpetuates inflammation [Biswas and Mantovani, 2010; Epstein et al., 1997]. It has been hypothesized that the aberrant regulation of the complex transcriptional factor NF-κB contributes to the development of pathogenic T cells in MS [Satoh et al., 2007] and it has been implicated in several autoimmune diseases and cancers[Boston University Biology, 2014].

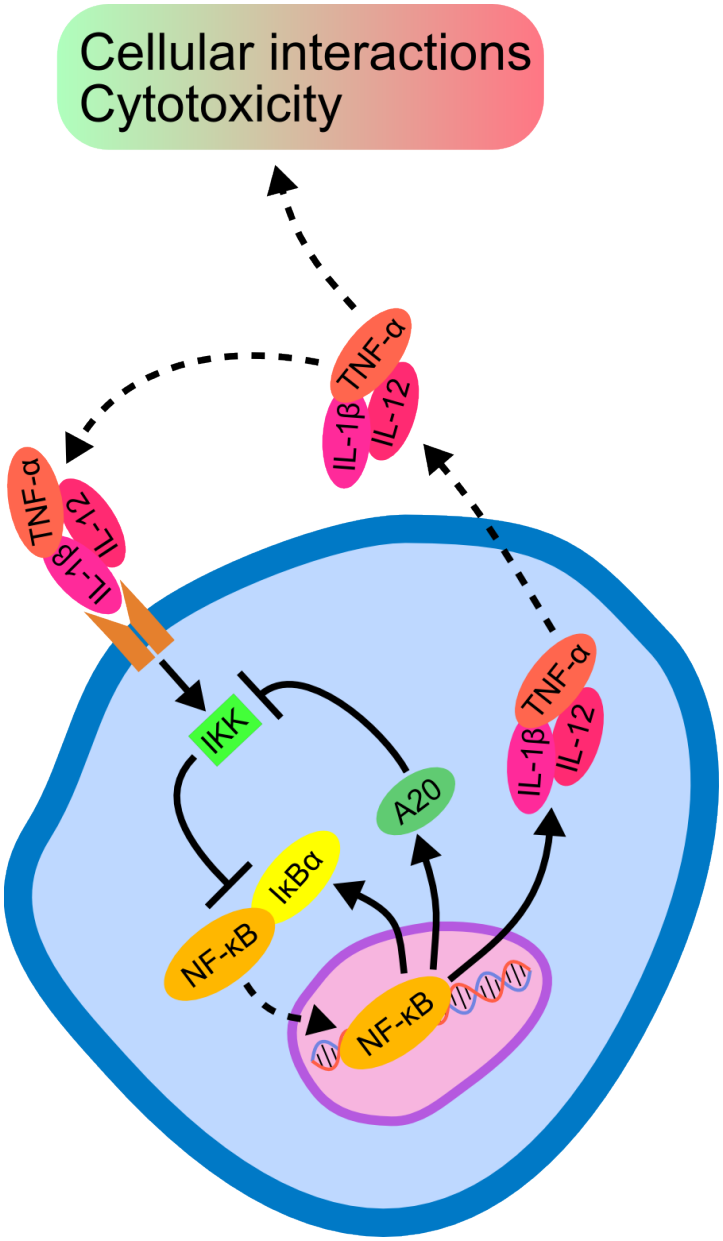

Figure 2.4: NF-κB auto-regulatory feedback loop inspired by [Biswas and Mantovani, 2010]. The process starts with the binding of cytokines like IFN-γ, TNF-α, or IL-1β onto M1 receptors. The receptor recruits Janus kinase adaptors, MyD88, and TRIF, inducing activation of the transcription factor NF-κB through the phosphorylation of the NF-κB-IκB complex by the IKK. This leads to the transcription of M1 genes, upregulating the production of pro-inflammatory cytokines like IL-12, TNF, and IL-1β, but also to the transcription of A20, an inhibitor of IKK, and more importantly IκBα. This activation results in a positive regulatory loop that amplifies and perpetuates inflammation[Biswas and Mantovani, 2010; Epstein et al., 1997].

3

Modeling Macrophages

"To be, or not to be – that is the essence of bistability."
– Rógvi Dávid Arge

Models of MS have been made with various approaches, some modeling it as an undirected fixed radius random graph[Mohan et al., 2008], and some, modeling baló's sclerosis, choosing to model it with a chemotactic approach, because of the formation of concentric patterns in the disease, and the formation of Liesegang rings in post-nucleation theories[Khonsari and Calvez, 2007]. In modeling MS, I had to chose between using T_h1 cells as the cells that perpetuate inflammation or using M1 macrophages. It has been shown that injection of autoimmune T cells into genetically susceptible animals induces experimental allergic/autoimmune enchephalomyelitis (EAE), which is an animal model of MS[Martin et al., 1992]. But due to initial suggestions, and due to evidence that the inactivation or downregulation of M1 macrophages, through mechanisms involving p38-, NF-κB-dependent signaling pathways, can result in resolving plaques[Starossom et al., 2012], this study focuses on adapting and applying a previously developed model using M1 macrophages as the main inflammatory cell.

In this chapter, a previous model of the interaction between cytokines and NF-κB will be modified and applied to a system of macrophages. The mathematical model will be explained and central terms in the model will be developed to give an understanding of them. The model and the biological system will be compared, to give argument for its applicability, and a comparison between the model and more general excitable media models will be made, to better understand the nature of the patterns appearing in the simulations.

3.1 Previous Model

The NF-κB activation process has been studied previously. A model was proposed by [Yde et al., 2011b], to describe potential cytokine waves in mammalian tissue based on the NF-κB signaling pathways as well as the bistable nature of the given biological system, to be able to describe the occurence of chronic inflammatory tissue. The application of the model to a chronic inflammatory system has been done previously by [Holst-Hansen], where it was applied to a group of α- and β-cells, called islets of Langerhans, in a quite succesful attempt to model observed phenomenon in diabetes. In the model, cytokine production through the upregulation of NF-κB was modeled by a a set of partial differential equations, where, N, R, T (T is replaced with I in this study), were the amounts of NF-κB, inhibitor, and TNF-α respectively:

$$\frac{\partial N}{\partial t} = k_{TN} \cdot f_N(T)(N_{tot} - N) - k_{RN} \cdot R \tag{3.1}$$

$$\frac{\partial R}{\partial t} = k_{NR} \cdot N - \frac{R}{\tau_R} \tag{3.2}$$

$$\frac{\partial T}{\partial t} = p \cdot f_T(N) - \frac{T}{\tau_T} + S, \tag{3.3}$$

where N_{tot} is the sum of passive and active NF-κB, and N is active NF-κB. Ignoring the fact that extracellular cytokines bind to a receptor and activate intracellular IKK, NF-κB is directly upregulated by the amount of extracellular cytokines, modelled by the activation function $f_N(T)$, and is proportional to the amounts of inactive NF-κB modelled by the $(N_{tot} - N)$. The inhibition of NF-κB is an intracellular process, and all inhibition is collected into the variable R as the amount of inhibitor and k_{RN} as the rate constant of this inhibition. Since NF-κB transcribes its own inhibitors the upregulation of NF-κB, also upregulates the production of inhibitors, here modelled by the terms $k_{NR}N$. Intracellular degredation and/or dilution of inhibitors is then the cause of downregulation of inhibitors, and is modelled by the term R/τ_R. The upregulation of NF-κB has the additional effect of upregulating the transcription of its own activators, namely some pro-inflammatory cytokines, like TNF-α and IL-1β. The amount of cytokines produced by the cell depends on the rate constant p as well as the activation function $f_T(N)$, which is a function of active NF-κB. The cytokines produced have a known half-life, and the downregulation of cytokines is here modelled by the degredation of them as T/τ_T. Lastly, an external stimulus is induced in the upregulation of cytokines by a constant S. In terms of autoimmune diseases, S can be interpreted as a defective cell or an infection, i.e. a cell that because of a defect or infection, doesn't recognise

the antibodies presented by regular cells, and therefore gets stimulated by normal healthy cells.

In [Yde et al., 2011a] the activation function for N and T, was the Hill function with a Hill coefficient of 3 for N and 2 for T.

$$f_N(T) = \frac{T^3}{T^3 + K_T^3}$$
$$f_T(N) = \frac{N^2}{N^2 + K_N^2}$$

where K_T, and K_N are thresholds for the activations of these to functions. The Hill function and Hill coefficient for N were chosen to match experimental observations [Yde et al., 2011a]. For T, the Hill function was chosen because NF-κB was reported to form dimers, but the study by [Yde et al., 2011a] also showed that replacing the Hill function with a linear activation function gave similar results.

The degradation of T and R, is proportional to the concentration of T and R respectively, where the constant of proportionality is the half-life $1/\tau_T$ for T and $1/\tau_R$ for R. This was chosen because the degradation may be carried out by dilution or proteasomes. As for the degradation of NF-κB and the production of inhibitors, these terms were based on Michaelis-Menten kinetics because of the relation to enzymatic bindings. A classical example of Michaelis-Menten kinetics is an enzyme catalyzing a substrate to create a product:

$$E + S \underset{k_r}{\overset{k_f}{\rightleftharpoons}} ES \xrightarrow{k_{cat}} E + P,$$

where E is enzyme, S is substrate, and P is product. Now assuming that the substrate S, is much larger than the Michaelis constant K_M[1], the change in product over time becomes:

$$\frac{d[P]}{dt} = k_{cat}\frac{E_{tot}[S]}{K_M + [S]} \approx k_{cat}E_{tot} \tag{3.4}$$

These derivations and assumptions are why the production rate of R and the inhibition rate of N are linear. A problem that does arise from

[1]The Michaelis constant is defined as:

$$K_M = \frac{k_{cat} + k_f}{k_r}$$

and can be derived from the steady-state to the time derivative of $[ES]$.

the linear terms is that the concentrations can become negative, which isn't the case for the nonlinear terms. Negative concentrations don't make sense physically and in the simulations they are set to zero. After all assumptions and choices of activation functions, the final equations are:

$$\frac{\partial N}{\partial t} = k_{TN}\frac{T^3}{T^3 + K_T^3}(N_{tot} - N) - k_{RN} \cdot R \tag{3.5}$$

$$\frac{\partial R}{\partial t} = k_{NR} \cdot N - \frac{R}{\tau_R} \tag{3.6}$$

$$\frac{\partial T}{\partial t} = p\frac{N^2}{N^2 + K_N^2} - \frac{T}{\tau_T} + S \tag{3.7}$$

By introducing parameter rescaling variables, we can reduce the number of parameters in the model. The rescaled variables are:

$$\tilde{N} = \frac{N}{N_{tot}} \tag{3.8}$$

$$\tilde{R} = \frac{R}{N_{tot}} \tag{3.9}$$

$$\tilde{T} = \frac{T}{K_T} \tag{3.10}$$

Giving the final form of their model:

$$\frac{\partial \tilde{N}}{\partial t} = k_{TN}\frac{T^3}{T^3 + 1}(1 - N) - k_{RN} \cdot R \tag{3.11}$$

$$\frac{\partial R}{\partial t} = k_{NR} \cdot N - \frac{R}{\tau_R} \tag{3.12}$$

$$\frac{\partial T}{\partial t} = p\frac{N^2}{N^2 + K_N^2} - \frac{T}{\tau_T} + S \tag{3.13}$$

The model for the production of cytokines through upregulation of NF-κB ends up having 8 parameters, k_{TN}, k_{RN}, k_{NR}, τ_R, p, K_N, τ_T, and S, where all but p and S are fitted to experimental data.
Lastly, by adding a diffusion term to eqn. (3.13)

$$\frac{\partial T}{\partial t} = p\frac{N^2}{N^2 + K_N^2} - \frac{T}{\tau_T} + S + D\nabla^2 T \tag{3.14}$$

they couple neighboring cells, making the development of cytokine waves possible.

3.1.1 Similarity to Macrophages

As was described in chapter 2, the inflammatory response in M1 macrophages are also a product of the NF-κB network. From figure 2.3 we see a simplified version of how recruitment of macrophages, and polarization of the

M1 phenotype, through the T_h1 cells is done. This system of interactions doesn't incorporate the details of the NF-κB network, and as a whole has to many interacting components to be feasible to model. Therefore, to be able to model the inflammatory response of M1 macrophages, we need some assumptions and simplifications.
First of all, as was stated in section 2.2.1, we are modeling recruitment and cellular interactions (see figure 2.3). This means we disregard the de- and remyelination phase of the inflammatory response. As for the recuitment of macrophages though they, like neutrophils, activate their own inflammatory response through TNF-α, their polarization into M1 macrophages, is done by the T_h1 cells, through the IL-12 $\rightarrow$ IFN-γ pathways [Janeway et al., 2001]. We are also assuming that M1 macrophages are readily available, i.e. there is no need for a recruitment and polarization of M0 macrophages by T_h1 cells. This eliminates the need for T_h1 cells. It also means that recruitment of M1 macrophages is done by the macrophages themselves, through the cytokines IL-12, IL-1β, and TNF-α. An additional assumption is that there are no M2 macrophages. This means that the only thing we are left with is M1 macrophages, that are self-activating and self-recruiting. From the full simplification scheme seen in figure 3.1, a set of components similar to the system described in [Yde et al., 2011a] appear.

Given that the simplified system is very similar to the model by [Yde et al., 2011a], adapting it to a system of static macrophages therefore becomes a matter of mapping the mathematics of their model to the simplified NF-κB network of the macrophages, and changing some of the free parameters to fit macrophages. What the model doesn't take into account is the chemotaxis of macrophages, which will be developed and described in section 3.1.3.

3.1.2 Applying and Modifying the Model

Macrophages and neutrophils both have a role to play in the inflammatory process, albeit different. Neutrophils are smaller, more numerous and have a shorter lifespan than the macrophage [Summers et al., 2010]. However, the chemokines and cytokines that activate chemotaxis and the inflammatory response in macrophages, also activate these processes in neutrophils. The longer lifespan of the macrophages make them ideal for inflammatory response simulations, where the focus lies on how the macrophages aggregate and what sort of patterns occur, since macrophage death can be disregarded, making the system simpler.

Furthermore, the study by [Vicker et al., 1986] on neutrophil accumulation showed that a constant spatial gradient of cytokines did not lead to chemotactic cell movement. The only way to induce chemotactic movement of neutrophils was through an impulse of chemoattractant, meaning that

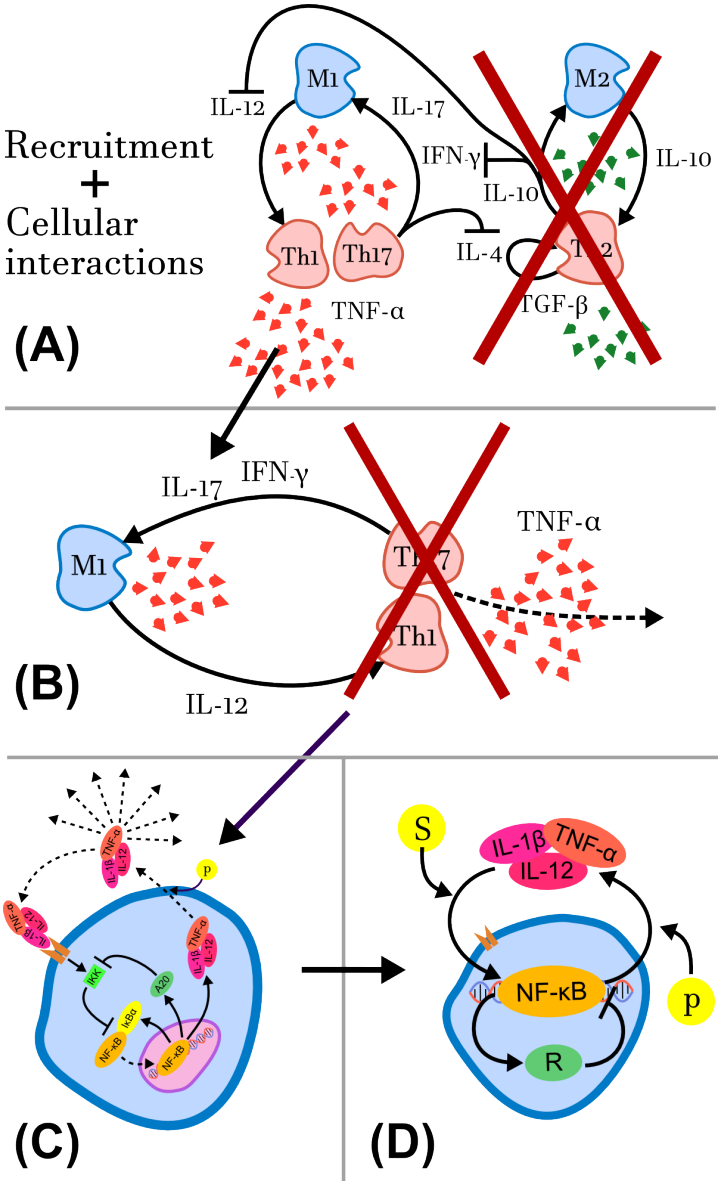

Figure 3.1: The simplifications used in this study to create a model of the NF-κB network of an M1 macrophage. **(A)** The recruitment and cellular interactions phase of figure 2.3. We assume that there are no M2 macrophages, T_h2 cells, and none of the cytokines produced by these. Since this study sets out to model the chemotactic movement of M1 macrophages, their inflammatory response, and their aggregation into plaques, at a timescale of up to 60 hours, this assumption is necessary to simplify the components of the system. **(B)** To simplify the system even further, we cut out the middle man, i.e. the T_h1- and T_h17 cells, and make macrophages responsible for their own recruitment. **(C)** A more detailed version of the inflammatory response of a macrophage, which illustrates a simplified NF-κB network. As a result of the simplification in **(B)**, this detailed version shows, macrophages as self-regulatory, with regards to the inflammatory response. **(D)** The final simplification of the system. This illustration shows how the extracellular cytokines, and intracellular inhibitors upregulate and downregulate the amount of active NF-κB in the cell respectively.

there is need of a temporal component to the chemoattractant. This result supports the use of the NF-κB model, as it gives rise to traveling cytokine waves given the right set of parameters.

The similarities between neutrophils and macrophages means that the equations developed for the NF-κB network of neutrophils can be directly applied to the macrophages, giving us the initial equations:

$$\frac{\partial N}{\partial t} = k_{IN} \cdot f_N(I)(N_{tot} - N) - k_{RN} \cdot R \tag{3.15}$$

$$\frac{\partial R}{\partial t} = k_{NR} \cdot N - \frac{R}{\tau_R} \tag{3.16}$$

$$\frac{\partial I}{\partial t} = p \cdot f_I(N) - \frac{I}{\tau_I} + S + D\nabla^2 I, \tag{3.17}$$

where T has been replaced I. The choice of activation functions for N was the Hill function, with a Hill coefficient of three, for the same reason as in section 3.1. For I, the activation function was chosen to be linear, as, [Yde et al., 2011a], had shown that a linear activation function qualitatively would result in the same response, as can also be seen in figure 3.2.

The equations can be simplified by redefining some variables, discretizing the spatial variables x and y, and non-dimensionalising the diffusion constant:

$$\tilde{N} = \frac{N}{N_{tot}} \tag{3.18}$$

$$\tilde{R} = \frac{R}{N_{tot}} \tag{3.19}$$

$$\tilde{x} = \frac{x}{d_{mp}} \tag{3.20}$$

$$\tilde{y} = \frac{y}{d_{mp}} \tag{3.21}$$

$$\tilde{D} = \frac{D}{d_{mp}^2} \tag{3.22}$$

$$\tilde{\nabla}^2 = (\frac{\partial^2}{\partial \tilde{x}^2} + \frac{\partial^2}{\partial \tilde{y}^2}) \tag{3.23}$$

where $\tilde{x} = \tilde{y} = 1$ cell, is the unitless grid size, and d_{mp} is the diameter of a macrophage. This leaves us with the final form of the PDE's:

$$\frac{\partial \tilde{N}}{\partial t} = k_{IN} \cdot \frac{\tilde{I}^3}{\tilde{I}^3 + 1}(1 - \tilde{N}) - k_{RN} \cdot \tilde{R} \tag{3.24}$$

$$\frac{\partial \tilde{R}}{\partial t} = k_{NR} \cdot \tilde{N} - \frac{\tilde{R}}{\tau_R} \tag{3.25}$$

$$\frac{\partial I}{\partial t} = p\tilde{N} - \frac{I}{\tau_I} + S + \tilde{D}\tilde{\nabla}^2 I, \tag{3.26}$$

To simplify the equations, the following redefinitions are used:

$$N \equiv \tilde{N} \tag{3.27}$$

$$R \equiv \tilde{R} \tag{3.28}$$

$$D \equiv \tilde{D} \tag{3.29}$$

$$\nabla^2 \equiv \tilde{\nabla}^2 \tag{3.30}$$

As for the values of the various rate constants, k_{IN}, k_{RN}, k_{NR}, and τ_R were fitted to match the initial peak of the NF-κB oscillations at around 30 minutes. The rate constants are $k_{IN} = k_{RN} = k_{NR} = 5\text{h}^{-1}$, and $\tau_R = 2\text{h}$. The half-life of the cytokine, is harder to choose, since they vary a whole lot depending on source and cytokine. For instance IFN-γ has a reported half-life of between $0.5 - 4.5$ hours [Ando et al., 2014], TNF-α a reported half-life of between $3 - 25$ minutes [Cheong et al., 2006], and for IL-1β the reported half-life is between $3 - 19$ minutes [Kudo et al., 1990]. The

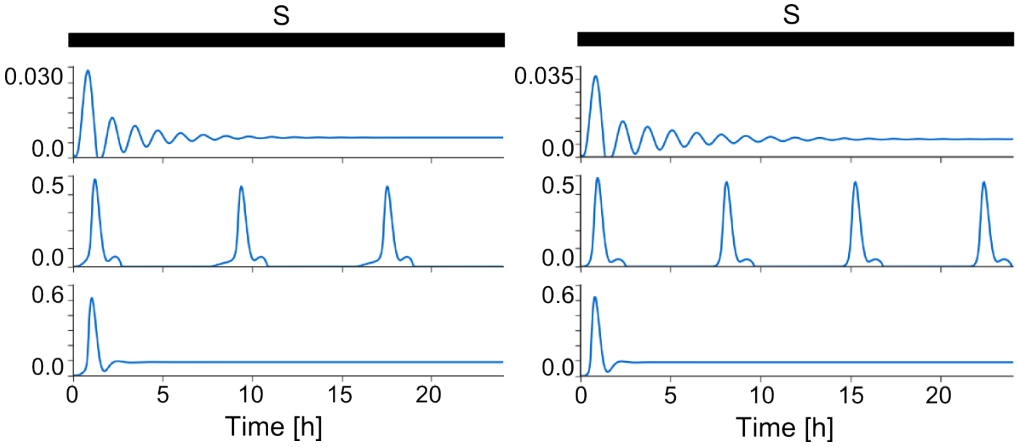

Figure 3.2: Dynamics of equations (3.24), (3.25), and (3.26) without diffusion. Illustrated here for NF-κB by running a simulation for 24 hours with a source term of $S = 1.0\text{h}^{-1}$ and $p = 2\text{h}^{-1}$ for the top row, $p = 46\text{h}^{-1}$ for the middle row, and $p = 90\text{h}^{-1}$ for the bottom row. **(LEFT)** Oscillations in NF-κB with Hill function as an activation function. **(RIGHT)** Oscillations in NF-κB with linear activation function.

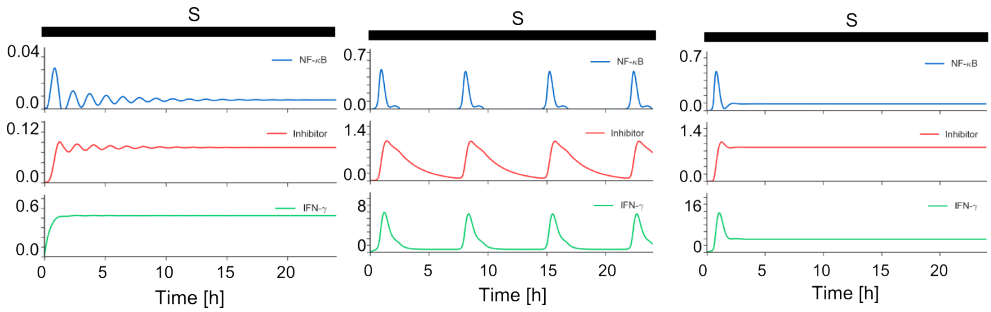

Figure 3.3: Dynamics of equations (3.24), (3.25), and (3.26) without diffusion. The figure shows the temporal development of NF-κB, inhibitor, and IFN-γ for various values of p. **(LEFT)** With $p = 2\text{h}^{-1}$ the system doesn't excite and is quite fast to find a very low steady state, with almost no production of cytokines. **(CENTER)** With $p = 46\text{h}^{-1}$ the system goes through spikes in cytokine production followed by a refractory period, where there is no production of cytokines because of the inhibitory effect on NF-κB is too high. **(RIGHT)** With $p = 90\text{h}^{-1}$ the system quickly finds a steady state with very high production of cytokines.

choice of cytokine half-life for this model was $\tau_I = 25$ min, which is at the upper end of TNF-α and IL-1β and at the lower end of IFN-γ. The study by [Yde et al., 2011a] also showed that a low $\tau_I < 0.5$ hours was necessary for the system to exhibit the three types of behaviour shown in figure 3.3, when changing the cytokine rate constant p. The study by [Goodhill, 1997] showed that diffusion of molecules like i.e. IL-1β, was of the order of $3 \cdot 10^{-7}\text{cm}^{-2}/\text{s}$, with an effective diffusion constant of approximately half. These results however, aren't known exactly for the brain, and e.g. the study by [Bendtsen et al., 2014] showed that the effective diffusion of the WRN protein was $D_{eff} \approx D/100$, which indicates that the effective diffusion constant could be much lower than half.

Running simulations, these equations are sufficient for a single stationary cell to exhibit behaviour ranging from no cytokine production to constant cytokine production as seen in figure 3.3.

3.1.3 Motile Macrophages

A novelty of this study is the addition of cell motility. In previous studies, people have looked at the spreading of cytokine waves and the bistable nature of a system of stationary cells, and how the geometry of cells can have a large effect on the spreading of cytokines and excitability of the system [Holst-Hansen]. But to be able to understand the accumulation of cells, and how cells are affected by a cytokine gradiant, one needs to take their motility into account.

Adding motility to a system of macrophages, though not to complex,

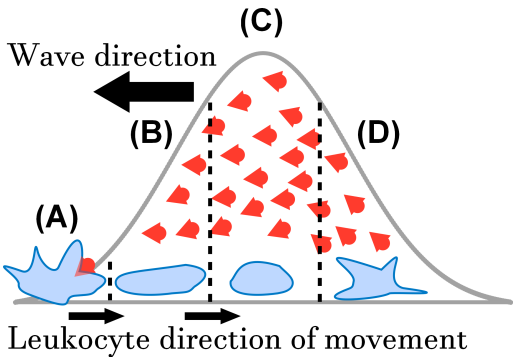

Figure 3.4: Figure inspired by figure 1.C in [Geiger et al., 2003]. It shows the one dimensional case of the four phases of leukocyte migration, introduced in [Geiger et al., 2003]. Take not that even though the direction on the figure is to the right, in a two dimensional space, the leukocyte moves deterministically along the positive cytokine gradiant[2], whilst moving like a random walker on the axis orthogonal to its movement. **(A)** the leukocyte registers a cytokine gradiant in a specific direction, **(B)** it then proceeds to rapidly move in the direction of the higher gradiant, **(C)**, when reaching a location where the cytokine gradiant stops increasing, the leukocyte stops moving, **(D)** the leukocyte gets ready to register cytokine gradiants again and awaits the next cytokine wave.

M-CSF
Macrophage colony-stimulating factor also known as M-CSF or CSF1, is a cytokine involved in the proliferation, differentiation, and chemotactic migration of various cells, macrophages being one of them.

Receptor-Mediated Endocytosis
Receptor-mediated endocytosis (RME), is the process by which a cell absorbs extracellular molecules by the invagination of the membrane vesicles containing proteins with the receptor sites specific to the molecules being absorbed.

introduces some uncertainties. The first issue is that movement speed of macrophages in the brain isn't known. In vitro experiments are of course good approximations to the real cellular environment, but they also introduce an uncertainty in the reported results. The second issue is that the various studies report different results for the velocity of macrophages. The study by [Vereyken et al., 2011] showed that the macrophage velocity was $0.003\mu m/s$, when moving toward a chemotactic signal. The study by [Grabher et al., 2007] however, showed that macrophages, moved at about 1μm/min, when moving randomly, while responding quickly to wounding, increasing their velocity to over 10μm/min. This study also showed that macrophages migrate like a random walker, with a favored direction governed by the cytokine gradient. This type of migration, called chemotaxis, is also supported by the study on leukocytes by [Geiger et al., 2003] which shows that leukocytes move randomly when not affected by cytokines, but when exposed to cytokines they have a four phase migration pattern as seen in figure 3.4.

In contrast to the study by [Geiger et al., 2003], the paper by [Jones, 2000] states that macrophages have a two phase movement, when influenced by the chemotactic cytokine M-CSF. Their statement is based on results from various papers [Boocock et al., 1989; Li and Stanley, 1991; Webb et al., 1996] and in short, it says that macrophages can only register cytokines once every $20-30$ minutes and will continue to move in the direction of the initially measured positive gradient, until it is able to register again. The biological explanation for this is that through stimulation and endocytosis

of all the M-CSF receptors, the macrophage is not able to sense any M-CSF until the M-CSF receptors are recycled to the surface, which is what [Boocock et al., 1989] show to be $20 - 30$ minutes. So to sum up, there are essentially two types of macrophage movement that have to be considered for the model:

1. Directed migration, deterministically moving towards a positive cytokine gradient, while moving like a random walker when not exposed to cytokines.

2. Directed migration, moving towards a higher cytokine level, with refractory sensing time, while moving like a random walker when not exposed to cytokines.

Because of the novelty of motility in an excitable media, I will develop the rules for both motility models. The first will be called **Wave Model** (WM), and the second **Receptor Model** (RM). However, because of initial results of the Wave model showed that it was inferior to the Receptor model, the model will only be mentioned here.

WM Chemotaxis

Now that the methods for chemotaxis has been chosen, we can start the formulation of a set of governing rules to be used for the Wavedependent model.

Using the information from the cited studies, it is known that macrophages move towards a positive cytokine gradient. This means that both the spatial, and temporal gradient has to be positive. Using $\mathbf{I}_t(x, y)$ as the value of cytokines at time t and position (x, y), the spatial cytokine gradient is defined as:

$$\nabla \mathbf{I}_t(x, y) = \left(\frac{\partial}{\partial x}\hat{\mathbf{x}} + \frac{\partial}{\partial y}\hat{\mathbf{y}} \right) \mathbf{I}_t(x, y) \tag{3.31}$$

The temporal gradient at a specific location (x, y) we can find by looking at the difference between cytokine levels at two time steps:

$$\nabla_t \mathbf{I}(x, y) = \mathbf{I}_t(x, y) - \mathbf{I}_{t-1}(x, y) \tag{3.32}$$

From these two equations, we can set up some rules that govern the chemotactic movement of macrophages:

I The spatial gradient should be greater than zero:

$$\nabla \mathbf{I}_t(x, y) > 0 \tag{3.33}$$

II The temporal gradient at the current position (x_c, y_c) should be greater than or equal to zero:

$$\nabla_t \mathbf{I}(x_c, y_c) \geq 0 \tag{3.34}$$

III The temporal gradient at the new position (x_n, y_n) should be greater than zero:

$$\nabla_t \mathbf{I}(x_n, y_n) > 0 \tag{3.35}$$

The first rule ensures that a macrophage under influence of cytokines always moves from a lower cytokine level to a higher cytokine level. But a spatial gradient in itself, is not sufficient for a macrophages to determine if the cytokines are moving towards it, or away from it as illustrated in figure 3.5.

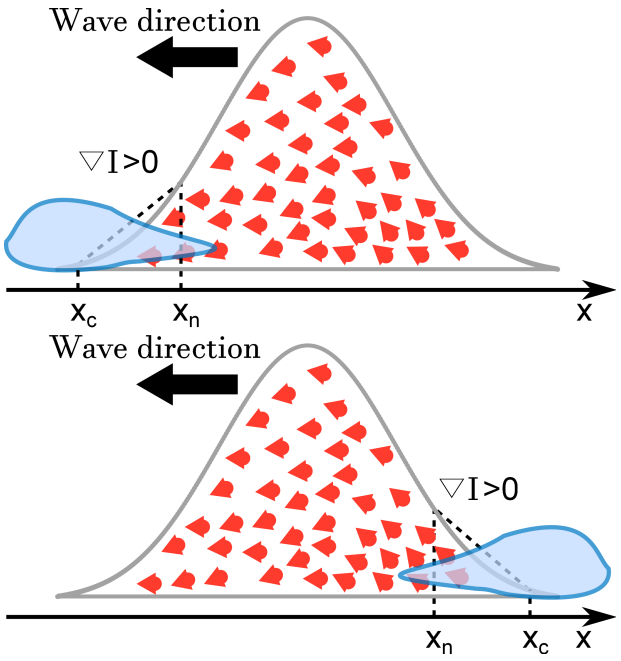

Figure 3.5: Illustration of why a spatial gradient isn't enough for macrophages to distinguish between positive or negative cytokine gradients.

Therefore, the second and third rules are needed. It ensures that increasing levels of cytokines are moving towards the macrophage and not away from it. The reason that II is allowed to be equal to zero is that the cytokine level at the position of the macrophage can be unchanged from one time step to the next. The reason it must be non-negative is that a temporal decreases in the local cytokine levels indicate a negative gradient, which means that the macrophages is on the back of the traveling wave.

RM Chemotaxis

For the RM macrophages are said to have cytokine receptors. These receptors get endocytosed when the macrophages measure a significant level of cytokines at a neighboring location. This significant level of cytokines is specified so that macrophages don't move with a directed motion towards every small increase in cytokine levels. Macrophages therefore only measure neighboring cytokine levels when the receptors are available. Macrophages still only move in a directed manner towards higher cytokine levels. This means that macrophage movement depends on the spatial gradient from equation (3.33). When a macrophage has measured a significant and higher level of cytokines at a neighboring location, its receptors get endocytosed. While they are being endocytosed, and before they are recycled to the cell surface, the macrophages move in the direction of the measured cytokine level. The time it takes macrophages to recycle the cytokine receptors is called $\tau_{Recycle}$ and is a value that is added to each macrophage.

Now that we have established a set of rules and attributes by which macrophages move chemotactically we finally have two finished models of the system and their implementation will be explained in the following chapter.

3.2 Macrophages as an Excitable Medium

The type of model we have introduced in this chapter, is called an Excitable Media model. These types of models are nonequilibrium systems with uniform rest states that are linearly stable, but are susceptible to pertubations. Excitable media are always in one of the following states: excitable, excited, and refractory. A good example of an excitable medium is forests and forest fires. A forest is initially in an excitable state. Given a spark, a fire is started and the trees that are on fire are said to be in the excited state. When the trees have burnt down, they become insusceptible to forest fires while they regrow. This period is called the refractory period. When the trees regrow, they become more and more susceptible to forest fires and the cycle can start again. Other examples of excitable media are the Belousov-Zhabotinsky reaction, the FitzHugh-Nagumo model, and the inflammatory response in neutrophils and β-cells. A necessety for an excitable medium is a fast positive feedback loop, a diffusing propagator, and a slowly or non-diffusing negative feedback loop. Using the forest fire example, the fast positive feedback loop is the fact that a small amount of spark can burst a tree into flame. The diffusing propagator is fire, and the slowly- or non-diffusing negative feedback loop is the regrowth or growth of trees.

Excitable media models with propagating waves can be described by using only two equations:

$$\partial_t u = f(u, v) + \nabla^2 u \tag{3.36}$$
$$\partial_t v = \epsilon g(u, v) + \delta \nabla^2 v, \tag{3.37}$$

where ϵ and δ are the fractional timescale difference and the fractional diffusion constant difference between u and v. The NF-κB model can be reduced to two variables and an analysis of the of a static system using the two variable NF-κB model has done by [Michelsen], but will not be done in this study.

From excitable media models, various wave patterns can appear, ranging from circularly traveling waves, spiral waves, and stationary localized pulses. In the following chapters we will see some of these types of patterns, as they appear under various conditions of the dynamic NF-κB model.

4

Computational Model

"Good news everyone!"
– Professor Farnsworth

Mathematical models and analytical solutions are not always enough to solve equations, when the problems get too complex. Instead, such equations, or systems are solved using numerical simulations and agent based modeling. In the previous chapter, a mathematical model for the production of and migration towards cytokines was developed. For a system of macrophages however, the complex interactions between diffusing cytokines, moving macrophages and intracellular activation/transcription of NF-κB, and production of inhibitor and cytokines, becomes too complex to find an analytical solution. To be able to solve these equations we turn to computer simulations and therefore need computational model, based on the equations and rules developed in the previous chapter, which will be used to generate simulation results in chapter 6.

The chapter will start by introducing the simulation setup and methods. Numerical solution of equation (3.26) will be shown, and lastly the development of a numerical model governing macrophage chemotaxis and random walk.

4.1 Simulation Setup and Methods

To solve the equations from the previous chapter, a program was written in C++, based on object-oriented principles, which solves equations (3.24), (3.25), and (3.26), but without diffusion, for each macrophage in the system using the 4'th order Runga-Kutta method (RK4). The spatial part of

equation (3.26), i.e. the diffusion, is solved for every grid cell in the system using the Euler method. Object-oriented programming was used to create each macrophage as a self-consistent object, meaning that each macrophage had a set of attributes, equations, and decision-making heuristics specific to that macrophage. The simulations were performed on a two dimensional quadratic grid of size $N_x = N_y = 200$, where each cell contained at most one macrophage as well as the concentration of cytokines. The macrophages were randomly distributed on the grid, and the amount of macrophages in the grid is based on a wanted density. For most of the simulations and if not specified, this value was chosen to be $\rho = 0.15$, meaning that 15% of the grid was filled with macrophages. This value was based on the number of average macrophages $\bar{m} = 350$ cells/mm^2 reported in [Nimmerjahn et al., 2005]. One macrophage had an additional production of cytokines, represented by S in equation (3.26), and this macrophage was always placed in the center. The simulations ran for a finite amount of time with a fixed timestep, and for each timestep the equations of the model for each macrophage were solved and each of the macrophages had to decide whether or not to move to one of the adjacent cells based on its decision-making heuristics. Furthermore, the data for each grid cell was written to files every tenth timestep. This included macrophages locations in the grid cell and the number of cytokines in that grid cell. The average NF-κB, inhibitor and cytokine data was also written to files. Python along with the modules, numpy, matplotlib, and seaborn are used to visualize the simulations, either in the form of movies showing the movement of the macrophages and the diffusion of cytokines, or in the form of plots showing the average levels of NF-κB, inhibitor, and cytokines over time.

Euler Method
An first order method for numerical integration of ordinary differential equations. It is easily derived Taylor expansion by ignoring higher than first order terms, is very fast to compute, but is less precise than higher order methods, and has an error term proportional to $\mathcal{O}(\Delta t)$.

Runga-Kutta
A family of numerical integration methods, for ordinary differntial equations. The higher order Runga-Kutta methods like the classical 4'th order Runga-Kutta, are slower to compute than the Euler method because of the many computations needed to calculate it, but is much more precise than the Euler method, with an error term proportional to $\mathcal{O}(\Delta t^4)$

4.1.1 Numerical Model

As was stated above, to solve the model equations, we need to make use of numerical integration methods. To solve the temporal part of the equations we use RK4. Given an equation and an initial value:

$$\frac{dI}{dt} = f(I,t) = pN + S - \frac{I}{\tau_I} \tag{4.1}$$

$$I(t_0) = I_0 \tag{4.2}$$

RK4 can mathematically formulated as:

$$I_{n+1} = I_n + \tfrac{\Delta t}{6}(k_1 + 2k_2 + 2k_3 + k_4) \tag{4.3}$$

$$t_{n+1} = t_n + \Delta t \tag{4.4}$$

with

$$k1 = f(I_n, t_n) \tag{4.5}$$
$$k2 = f(I_n + \frac{\Delta t}{2} k_1, t_n + \frac{\Delta t}{2}) \tag{4.6}$$
$$k3 = f(I_n + \frac{\Delta t}{2} k_2, t_n + \frac{\Delta t}{2}) \tag{4.7}$$
$$k4 = f(I_n + \Delta t k_3, t_n + \Delta t) \tag{4.8}$$

In this model, none of the variables N, R, and I, are independent, therefore to solve for one of them, we must solve for all of them. In terms of the RK4 method, this means that the computation of all k_1 for all the variables must be computed before computing k_2 and so forth. This is a timeconsuming process, but because of the smaller error of the RK4, it allows for much greater timesteps than the Euler method as seen in figure 4.1.

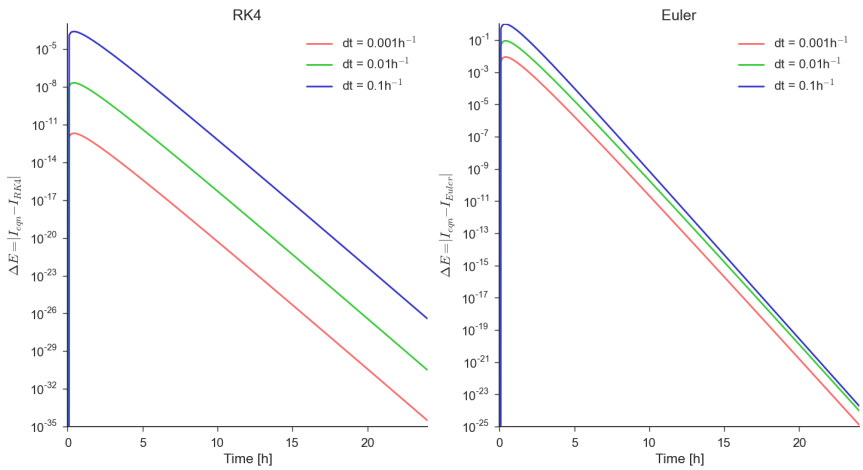

Figure 4.1: Difference in numerical errors of the two methods, RK4 and Euler. The equation solved was the temporal derivative of I, with an initial value of $I_0 = 20$, no source $S = 0$, and no diffusion $D = 0$. The exact solution to this equation is $I(t) = I_0 exp(-t/\tau_I)$.

To solve the diffusion and decay part of equation (3.26), we use the Euler method for the time integration. Solving the diffusion term is a matter of Taylor expanding I around all the positions $(x \pm \Delta x, y)$, $(x, y \pm \Delta y)$, and $(x \pm \Delta x, y \pm \Delta y)$. The Taylor expansion of these, and their recombinations are called the Forward-, Backward- and Central Difference methods, where the first two are first order accurate in space, while the last is second order accurte in space. To ease the writing, I redefine $x \equiv i$, $y \equiv j$, and use the nondimensionalized grid cell distances $\Delta x = \Delta y = 1$, and the diffusion term $D = D/d_{mp}^2$. The resulting solution to the diffusion term for the Moore

neighborhood is:

$$D\nabla^2 I = A\frac{D}{\Delta x^2}(I_{i+1,j} + I_{i-1,j} + I_{i,j+1} + I_{i,j-1} - 4I_{i,j}) \tag{4.9}$$

$$+ \frac{B}{2}\frac{D}{\Delta x^2}(I_{i+1,j+1} + I_{i+1,j-1} + I_{i-1,j+1} + I_{i-1,j-1} - 4I_{i,j}), \tag{4.10}$$

where we have used that $\Delta x = \Delta y = 1$ and with the condition that $A+B = 1$. The time derivative of I, in terms of the Euler method is written as:

$$\frac{\partial I}{\partial t}\Big|_{i,j,t} \approx \frac{I_{i,j,t+\Delta t} - I_{i,j,t}}{\Delta t} \tag{4.11}$$

can then be used to find the solution of $\frac{\partial I}{\partial t}$ at time $t = t+\Delta t$, and is written as:

$$I_{i,j,t+\Delta t} = I_{i,j,t} + \frac{D\Delta t}{2\Delta x^2}(I_{i+1,j} + I_{i-1,j} + I_{i,j+1} + I_{i,j-1} - 4I_{i,j}) \tag{4.12}$$

$$+ \frac{D\Delta t}{4\Delta x^2}(I_{i+1,j+1} + I_{i+1,j-1} + I_{i-1,j+1} + I_{i-1,j-1} - 4I_{i,j}), \tag{4.13}$$

where $A = B = \frac{1}{2}$ and the numerical solution is first order accurate in time and second order accurate in space. The validity of our numerical solution depends on how well it corresponds to the exact solution in the limit of $\Delta t \to 0$ and $(\Delta x, \Delta y) \to (0, 0)$. If this is the case, we say that our numerical approximation converges, and thus we can say that our simulations approximate the exact solution. The Lax Equivalence Theorem states that for a consistent finite difference method for well-posed linear initial value problem, the method converges if and only if it is stable. The necessary stability condition for this equation is:

Moore neighborhood The Moore neighborhood is a definition of neighboring cells from the discrete computational model called Cellular Automaton. It is defined as the eight closest adjacent cells, and differs from the von Neumann neighborhood which only includes the four closest adjacent cells.

$$2D\Delta t + D\Delta t \leq 1 \tag{4.14}$$

$$\Delta t \leq \frac{1}{3D} \tag{4.15}$$

This means that the choice of stepsize is upper bounded by the size of the diffusion term. So far, these proofs and conditions make the choice of a low stepsize preferable as it makes the solution more correct. But because smaller Δt means that we need to do more computations to reach the end of the simulation, the accumulation of small errors can become higher than the larger errors of a higher Δt. This leads to a tradeoff between truncation error, error by high Δt, and roundoff error, error by many computations. In section 3.1.2 the diffusion constant of the cytokine IL-1β is stated to be $D = 3 \cdot 10^{-7}\text{cm}/s$. Non dimensionalizing this value and using it in equation (4.15), we get $\Delta t \leq 1/3D = 1/(3 * 244.9)\text{h} = 0.001\text{h}$.

4.1.2 Computational Model

As was stated above, macrophages move like random walkers, when not affected by any cytokines, but still use their filopodia to scan the environment. The ability of macrophages to move, is programmed to be a function of the macrophage class, and is called at every timestep. The new location that the macrophage evaluates is chosen at random from one of eight possible moves and how the location is evaluated will now be specified.

Random Walk

The Random Walk is specified in 1D as such: For each timestep Δt, the particle at position x_i, makes a move along the positive x-axis, with probability $1/2$ and along the negative x-axis with probability $1/2$. This approach however, must be modified for the model because the macrophages have a velocity, i.e. an average distance traveled per hour. In section 3.1.3, we specified some movement speeds in the units μm/h, but in the simulations, the grid will be non-dimensionalized into unit spacing, and therefore the velocity of the macrophages must be non-dimensionalized as well. Dividing the reported velocities with the diameter of the macrophage, we get the macrophage random walk velocity and chemotaxis velocity:

$$v_{mp,RW}^{vereyken} = 0.51 \text{ cells/h} \tag{4.16}$$

$$v_{mp,RW}^{grabher} = 2.9 \text{ cells/h} \tag{4.17}$$

$$v_{mp,CT}^{grabher} = 28.6 \text{ cells/h} \tag{4.18}$$

where the values of $v_{mp,RW}$ and $v_{mp,CT}$, are the velocity of macrophages when they are- and aren't affected by cytokines respectively. Because only the study by [Grabher et al., 2007], reported velocities for both random walk and chemotaxis, these values will be used in the upcoming simulations. To enforce this in a random walk scenario, we can implement a movement probability. This means that the macrophage won't move at every timestep, but that its mean number of moves per hour will still be close to the velocity. An easy way of implementing a movement probability is to say that the macrophage moves if some random variable $p \in [0, 1]$ is smaller than $v_{mp}\Delta t/d$, where d, is the distance from (x_c, y_c) to (x_n, y_n). Because of unit spacing, in the grid the distance from a cell to its von Neumann neighborhood is $d = 1$, while the distance to the four cells at $x_{i\pm1,j\pm1}$ is $d = \sqrt{2}$. Using this information, we can write up a probability of movement for when macrophages aren't affected by cytokines:

$$P_{RW} = \frac{v_{mp,RW}\Delta t}{d} \tag{4.19}$$

Then for each timestep, if the macrophage isn't affected by cytokines, it will move with probability P_{RW}, in one of the eight possible directions. Adding velocity to the system, and using a probabilistic movement, we need to make sure that the probability of movement isn't greater than 1. In addition to satisfying equation (4.15), Δt now also has to satisfy the following inequality:

$$1 > \frac{v\Delta t}{d} \tag{4.20}$$

$$\tag{4.21}$$

This condition has to hold for all d. Setting d to its lowest value $d = 1$ gives:

$$1 > v\Delta t \tag{4.22}$$

$$\Delta t < \frac{1}{v} \tag{4.23}$$

Using the highest reported velocity in this equation we get $\Delta t < \frac{1}{28.6}\text{h} = 0.035\text{h}$. This upper bound on Δt is higher then the one obtained from equation (4.15), but as was stated in section 3.1.2, the effective diffusion constant could be up to 100 times lower than the diffusion constant. This affects the upper bound on Δt found from equation (4.15) making it as high as $\Delta t < 0.136\text{h}$. So to clarify, the timestep Δt is upper bounded by the lower value found from the two equations (4.15) and (4.23).

Receptor Model

For the RM we add a receptor recycling time for each macrophage. We will call this variable $\tau_{Recycle}$ and the recycling time is chosen to be in the $20 - 30$ minute interval specified in the paper by [Jones, 2000]. To make all the macrophages receptor recycling time be in this interval, the variable $\tau_{Recycle}$ is defined as:

$$\tau_{Recycle} = (20 + dU)/60 \text{ h}^{-1} \tag{4.24}$$

where dU is a random number drawn from the uniform distribution $U(A, B)$ where A and B are the upper and lower bounds of the distribution. To ensure that each macrophages' receptor recycling time is between 20 minutes and 30 minutes the lower and upper bound are chosen to be $A = 0$ minutes and $B = 10$ minutes, giving an ensemble mean recycling time of $\langle\tau_{Recycle}\rangle = 25/60 \text{ h}^{-1}$. For each timestep macrophages evaluate one of eight possible directions. If the evaluated locations' cytokine levels are significant ($I > 0.05$) and greater than the current locations cytokine levels, a timer, $T_{Recycle}$ is set to the value of that specific macrophages' $\tau_{Recycle}$. While this

counter is greater than zero, the macrophage will not evaluate its neighboring cells' cytokine levels but will move in the same direction as previously with probability $P = \frac{v_{mp,CT}\Delta t}{d}$. The movement probability is again added to ensure that the mean moves per hour is $v_{mp,CT}$. The computational steps for this model should be understood as follows:

- Evaluate the randomly chosen new locations current cytokine levels
- If the receptors are available, i.e. $T_{Recycle} \leq 0$, then
  - If the new locations cytokine levels are significant and higher, move with a probability of $P = \frac{v_{mp,CT}\Delta t}{d}$ to the new location, set a receptor recycling timer to be equal to $T_{Recycle} = \tau_{Recycle}$, and save the direction of the move.
  - Else move with probability P_{RW} to the new location.
- Else with probability $P = \frac{v_{mp,CT}\Delta t}{d}$ move in the direction of the previous move, and decrease the receptor recycling timer by the size of the timestep $T_{Recycle} = T_{Recycle} - \Delta t$

This model allows the macrophages to move like random walkers when not affected by cytokines, and to move in a specific direction when there is a cytokine pulse/wave and when the cytokine receptors are available.

We now have all that we need to run simulations for motile excitable media, but first we will do a short analytical analysis of the stationary model, to illustrate the bistability of the system.

5

Model Analysis

"Chaos was the law of nature; Order was the dream of man."
– Henry Adams

So far the focus of this study has been understanding the biological and physiological system, and developing a mathematical- and computational model for the production of and migration towards cytokines in a population of macrophages. In chapter 3 a model for the production of cytokines was developed, and we can now with simulations show how such a system behaves under various conditions. But first, we will take an analytical approach, to see what can be derived from the model.

This will be a short chapter with an analytical analysis of equations (3.24), (3.25), and (3.26), for a stationary macrophage showing the bistability of the system and the evolution of the variables in phase space [1].

5.1 Stationary Macrophage

For the analytical approach, we will assume that we have a single immovable macrophage, and that cytokines do not diffuse. We will look at the solutions to the steady-states of the model equations, and from this see the bistable nature of the model. The effect of our free parameter p, will be analysed, and bifurcation of the steady-state solutions as a function of p will be shown. Furthermore we will look at the effect of S on the system, and show how it can be used to lower the critical p needed for excitability.

[1] This has been done very thouroughly in [Holst-Hansen, Chapter 4. Model Analysis] and thus I highly recommend interested readers to read it.

5.1.1 Steady State

To show the bistability of the model, we can look at the solution to equations (3.24), (3.25), and (3.26) in steady state.

$$0 = k_{IN}\frac{I_{ss}^3}{I_{ss}^3+1}(1-N_{ss}) - k_{RN}R_{ss} \tag{5.1}$$

$$0 = k_{NR}N_{ss} - \frac{R_{ss}}{\tau_R} \tag{5.2}$$

$$0 = pN_{ss} - \frac{I_{ss}}{\tau_I} + S + \nabla^2 I_{ss} \tag{5.3}$$

Equations (5.1) and (5.2) can be combined to get the steady state for N:

$$R_{ss} = k_{NR}\tau_R N_{ss} \tag{5.4}$$

$$N_{ss} = \frac{I_{ss}^3}{I_{ss}^3(\alpha+1)+\alpha} \tag{5.5}$$

with $\alpha = \frac{k_{RN}k_{NR}\tau_R}{k_{IN}}$. As for the steady state of equation (5.3) we neglect the source and the diffusion term, and hence get the steady state solution

$$I_{ss} = p\tau_I N_{ss} \tag{5.6}$$

which after inserting the steady-state solution for N, becomes:

$$I_{ss} = p\tau_I \frac{I_{ss}^3}{I_{ss}^3(\alpha+1)+\alpha} \tag{5.7}$$

which has the trivial solution $I_{ss} = 0$. Rewriting it, we get the third order polynomial:

$$(1+\alpha)I_{ss}^3 - p\tau_I I_{ss}^2 + \alpha = 0 \tag{5.8}$$

Solving this equation directly is hard, but by making some assumptions, and using a few tricks, we can easily find approximate solutions to this equation. First, we rewrite the equation:

$$p\tau_I - (1+\alpha)I_{ss} = \alpha I_{ss}^{-2} \tag{5.9}$$

$$\frac{\alpha}{\alpha+1}I_{ss}^{-2} = \frac{p\tau_I}{\alpha+1} - I_{ss} \tag{5.10}$$

$$\tag{5.11}$$

Assuming that I_{ss} is very high, the left side of equation (5.10) is approximately zero, and thus, we have a steady-state when $I_{ss} = \frac{p\tau_I}{\alpha+1}$. Rewriting

the equation, we can find the last solutions:

$$\begin{aligned} I_{ss}^{-2} &= \frac{\alpha+1}{\alpha}\left(\frac{p\tau_I}{\alpha+1} - I_{ss}\right) \\ I_{ss}^{2} &= \frac{\alpha}{\alpha+1}\left(\frac{p\tau_I}{\alpha+1} - I_{ss}\right)^{-1} \\ I_{ss}^{2} &= \frac{\alpha}{p\tau_I}\left(1 - \frac{\alpha+1}{p\tau_I} I_{ss}\right)^{-1} \end{aligned} \tag{5.12}$$

Taylor expanding the term around $x = 0$ in the parenthesis to first order gives $(1-x)^{-1} \approx 1+x$, where $x = \frac{\alpha+1}{p\tau_I}$, from which we get the second order polynomial:

$$\begin{aligned} I_{ss}^{2} &\approx \frac{\alpha}{p\tau_I}\left(1 + \frac{\alpha+1}{p\tau_I} I_{ss}\right) \\ 0 &= I_{ss}^{2} - \frac{\alpha(\alpha+1)}{p^2\tau_I^2} I_{ss} - \frac{\alpha}{p\tau_I} \end{aligned} \tag{5.13}$$

This gives the solutions:

$$\begin{aligned} I_{ss} &= \frac{\frac{\alpha(\alpha+1)}{p^2\tau_I^2} \pm \sqrt{\left(\frac{\alpha(\alpha+1)}{p^2\tau_I^2}\right)^2 + 4\frac{\alpha}{p\tau_I}}}{2} \\ &= \frac{\alpha(\alpha+1) \pm \sqrt{\left(\alpha(\alpha+1)\right)^2 + 4\alpha p^3\tau_I^3}}{2p^2\tau_I^2} \end{aligned} \tag{5.14}$$

Giving us the steady-state solutions, also called fixed-points:

$$I_{ss,1} = 0 \tag{5.15}$$

$$I_{ss,2} = \frac{\alpha(\alpha+1) \pm \sqrt{\left(\alpha(\alpha+1)\right)^2 + 4\alpha p^3\tau_I^3}}{2p^2\tau_I^2} \tag{5.16}$$

$$I_{ss,3} = \frac{p\tau_I}{\alpha+1} \tag{5.17}$$

To find out which of these solutions are stable, we compute the Jacobian. We can then compare the determinant and the trace of the Jacobian evaluated at the biologically valid steady-states, i.e. non-negative solutions since concentrations have to be positive [Strogatz, 2014]. The Jacobian of our system is defined as such:

$$\mathbf{J} = \begin{pmatrix} \frac{\partial \dot{N}}{\partial N} & \frac{\partial \dot{N}}{\partial R} & \frac{\partial \dot{N}}{\partial I} \\ \frac{\partial \dot{R}}{\partial N} & \frac{\partial \dot{R}}{\partial R} & \frac{\partial \dot{R}}{\partial I} \\ \frac{\partial \dot{I}}{\partial N} & \frac{\partial \dot{I}}{\partial R} & \frac{\partial \dot{I}}{\partial I} \end{pmatrix} \tag{5.18}$$

Which after some derivations becomes:

$$\mathbf{J} = \begin{pmatrix} -k_{IN}I^3/(I^3+1) & -k_{RN} & k_{IN}(1-N)3I^2/(I^3+1)^2 \\ k_{NR} & -1/\tau_R & 0 \\ p & 0 & -1/\tau_I \end{pmatrix} \tag{5.19}$$

To find the stability of a fixed point, we can check the sign of the real part of the eigenvalues. If they are all less than zero, the fixed point is stable and if one or more of them are positive, the solution is unstable. The eigenvalues of the Jacobian are found from the equation:

$$\det|\mathbf{J} - \lambda\mathbb{I}| = 0, \tag{5.20}$$

where $\mathbb{I}$ is the identity matrix. Plugging in the steady-state solutions from equations (5.15), (5.28), and (5.17), and using the values $k_{IN} = k_{RN} = k_{NR} = 5$ h^{-1}, $\tau_R = 120/60$ h^{-1}, $p = 140$ h^{-1}, and $\tau_I = 25/60$ h^{-1} for the model parameters, we get the following eigenvalues:

$$\begin{array}{lccc} I_{ss,1} \Rightarrow & \lambda_1 = -2.4 & \lambda_2 = -\frac{1}{4} + 4.99i & \lambda_3 = -\frac{1}{4} - 4.99i \\ I_{ss,2} \Rightarrow & \lambda_1 = -19.03 & \lambda_2 = 16.11 & \lambda_3 = -0.35 \\ I_{ss,3} \Rightarrow & \lambda_1 = -2.6 + 4.18i & \lambda_2 = -2.6 - 4.18i & \lambda_3 = -2.67 \end{array}$$

From these eigenvalues, we can deduce that $I_{ss,1}$, and $I_{ss,3}$ are stable nodes, and $I_{ss,2}$ is a saddle point. This is exactly what we wanted the model to exhibit, because it means that the stable steady-states, are when the concentration of I is either high, or low, while it has an unstable fixed point in between. The steady-states can be seen as filled (stable) or empty (unstable) rings in figure 5.1, where the arrows represent the direction field, which are calculated from the instantaneous value of $\frac{\partial N}{\partial t}$, and $\frac{\partial I}{\partial t}$, at various values of N and I.

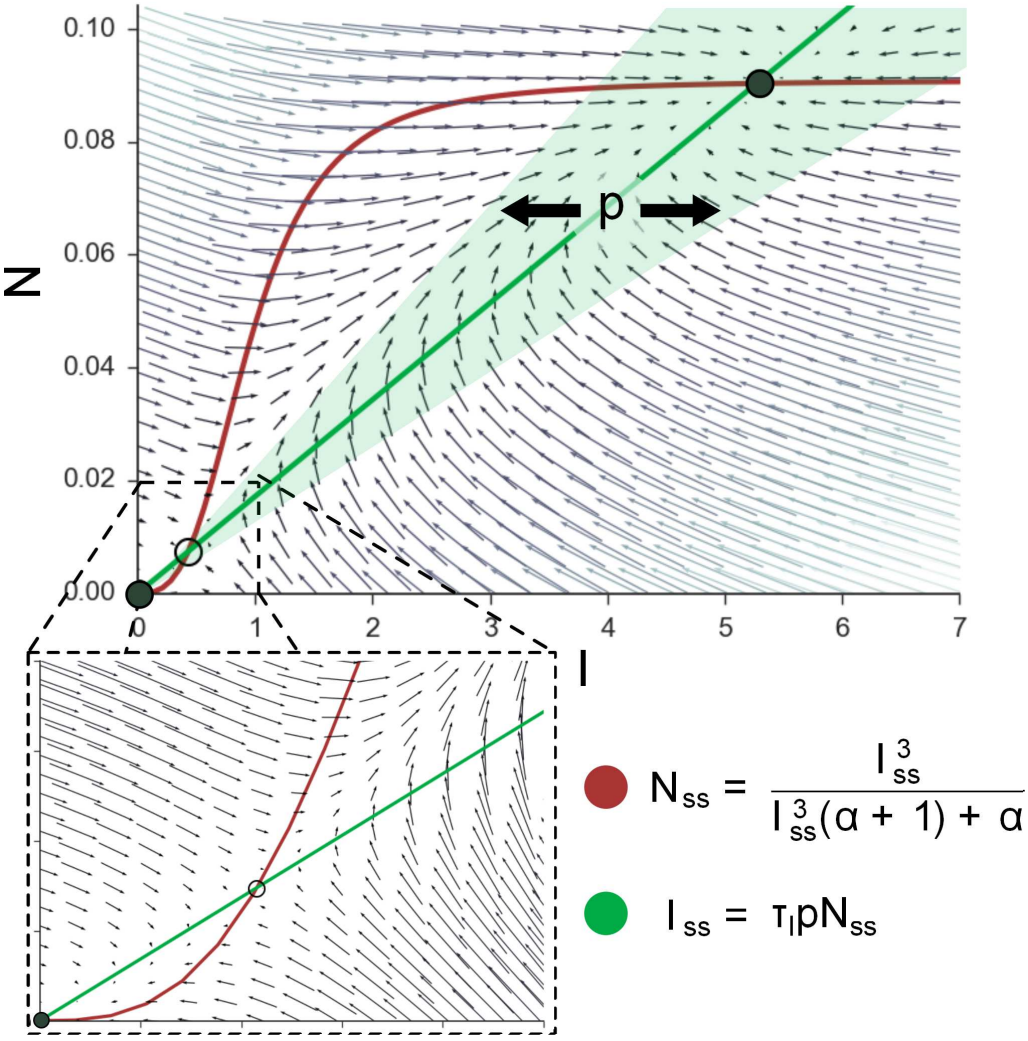

Figure 5.1: $I - N$ phase space illustration of the bistability of the model for $p = 140$ h^{-1}, at the steady-state level of R. Filled rings are the stable steady-state solutions to equation (5.8), while the open ring is an unstable solution. The arrows represent the direction field, and serve to illustrate the point that the low and high concentrations of I, are stable nodes, while the intermediate fixed point is a saddle point.

The bistability of this model is highly dependent on the value of p, where a too low value of p will result in the only stable solution being the zero point.

5.1.2 Critical p

To illustrate the point made in the last section, that the bistability of the model is highly dependent on the value of p, we will take the analytical approach to show the bifurcation point as a function of p. To do this, we

can use equation (5.7), and write up p as a function of I:

$$p(I) = \frac{I^3(\alpha+1)+\alpha}{\tau_I I^2} \tag{5.21}$$

The critical p value is found as the minimum $I_{min} \neq 0$, that is a solution to $\frac{dp}{dI} = 0$, i.e. we want to find a local extrema of p as a function of I (see figure 5.2). Differentiating $p(I)$ with respect to I, we get:

$$\frac{dp}{dI} = \frac{I^3(\alpha+1)-2\alpha}{\tau_I I^3} = 0 \tag{5.22}$$

The only non-zero solution to this equation is found by looking at the numerator:

$$I^3(\alpha+1) = 2\alpha \tag{5.23}$$

$$I = \left(\frac{2\alpha}{\alpha+1}\right)^{1/3} \tag{5.24}$$

Inserting this into equation (5.21), and using the specified variable values, we find that the critical p is:

$$p(I_c) = \frac{I_c^3(\alpha+1)+\alpha}{\tau_I I_c^2} \tag{5.25}$$

$$p_c = p(I_c) = 48.3 \text{ h}^{-1} \tag{5.26}$$

The bifurcation point, and some resulting $I-N$ phase-plane steady-states can be seen in figure 5.2.

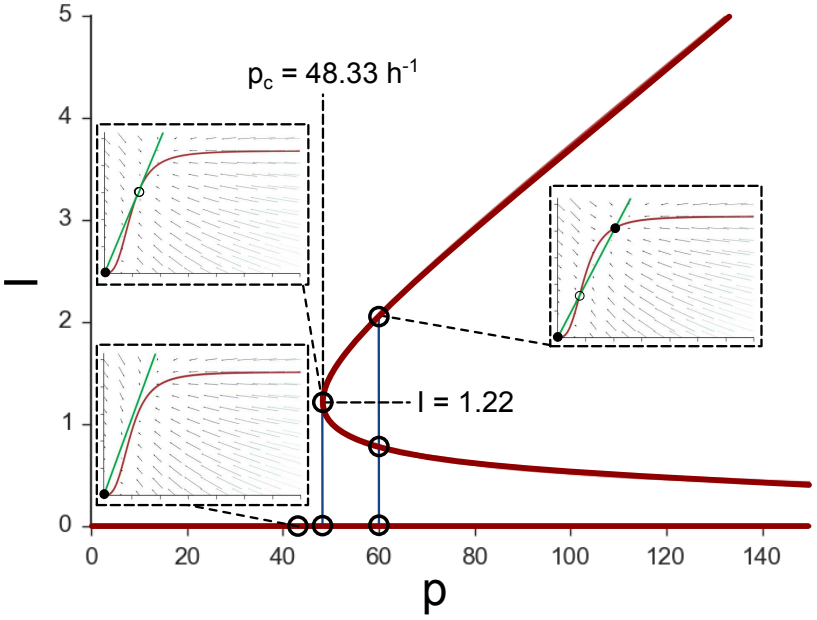

Figure 5.2: $I-p$ phase plane analysis, showing the steady-state solutions to equation (5.8), along with three $I-N$ phase-plane plots for various values of p.

The meaning of this bifurcation point, is that below p_c, there is only one fixed point, and the macrophage can't get excited. Above p_c, the macrophage can, if I gets large enough, stabilize in an excited level. This excited stable state is what we will call the chronic inflammatory state (CIS). Using this result as inspiration, we can hypothesis about how, a CIS can be alleviated. From figures 5.1, and 5.2, we can see that, to go from the CIS to the healthy state (HS), we can do one of three things:

1. Lower I
2. Lower p
3. Lower N
4. Increase R

Since I is extracellular, lowering it could be done by lowering the lifetime of cytokines τ_I. Biologically, this would mean either increasing the uptake of cytokines by other cells, or breaking down the cytokines using enzymes. Lowering of I, could indirectly also be done by lowering p. Because p, is of loose biological meaning, it is hard to say, what the biological equivalence is of lowering it. However, it is still an interesting thought, because computationally, this is a very simple thing to do, which makes analysing it easy. The last thing one could do, is lowering N. Since N is intracellular, lowering N, would mean either increasing the effect of inhibitors on N, either by increasing the effect of R on N, or N on R, or lowering the effects of cytokines. Lowering the effects of cytokines on the NF-κB production is the most appealing method, as a study by [Starossom et al., 2012] showed that downregulation of M1 macrophages through p38-, and NF-κB signaling pathways, could result in resolving plaques. In the model, a lowering of the positive feedback parameter k_{IN} is rather straight forward, but the biological meaning of this could be interpreted in different ways. One way to interpret it, is that an inhibitor is introduced to the system, that blocks some of the cytokine receptors on the macrophages. This would lead to a lower uptake of I, and result in a lower N. Another way to interpret it is inspired by the study by [Starossom et al., 2012]. In the study the introduction of GAL1 significantly decreased the phosphorylation of p38, and IκB-α. Because k_{IN} in the model, effectively is the phosphorylation of IκB-α, this result is very interesting, and will be analysed in the following chapter.

GAL1
Encoded by the LGALS1 gene, Galectin-1 is a protein implicated in the regulation of innate and adaptive immunity. It is part of the family of endogenous lectins, who function in the extracellular environment by interacting with many glycosylated receptors. Recent evidence, suggests that they also play a role in modulating the intracellular signaling pathways[Starossom et al., 2012].

5.1.3 Defective Macrophage

As was explained in section 3.1 a defective macrophage gets an additional term S. The purpose of this term, is to instigate the cytokine production,

thereby starting the inflammatory process. But what effect does this term have on the critical p, and on the steady-state solutions of I? First of all, because we no longer are disregarding S, the steady-state equation for I becomes:

$$I_{ss} = p\tau_I \frac{I_{ss}^3}{I_{ss}^3(\alpha+1)+\alpha} + S\tau_I \tag{5.27}$$

Rewriting this equation, we get the fourth order polynomial:

$$I_{ss}^4(\alpha+1) + \alpha I_{ss} - p\tau_I I_{ss}^3 - S\tau_I I_{ss}^3(\alpha+1) + S\tau_I\alpha = 0 \tag{5.28}$$

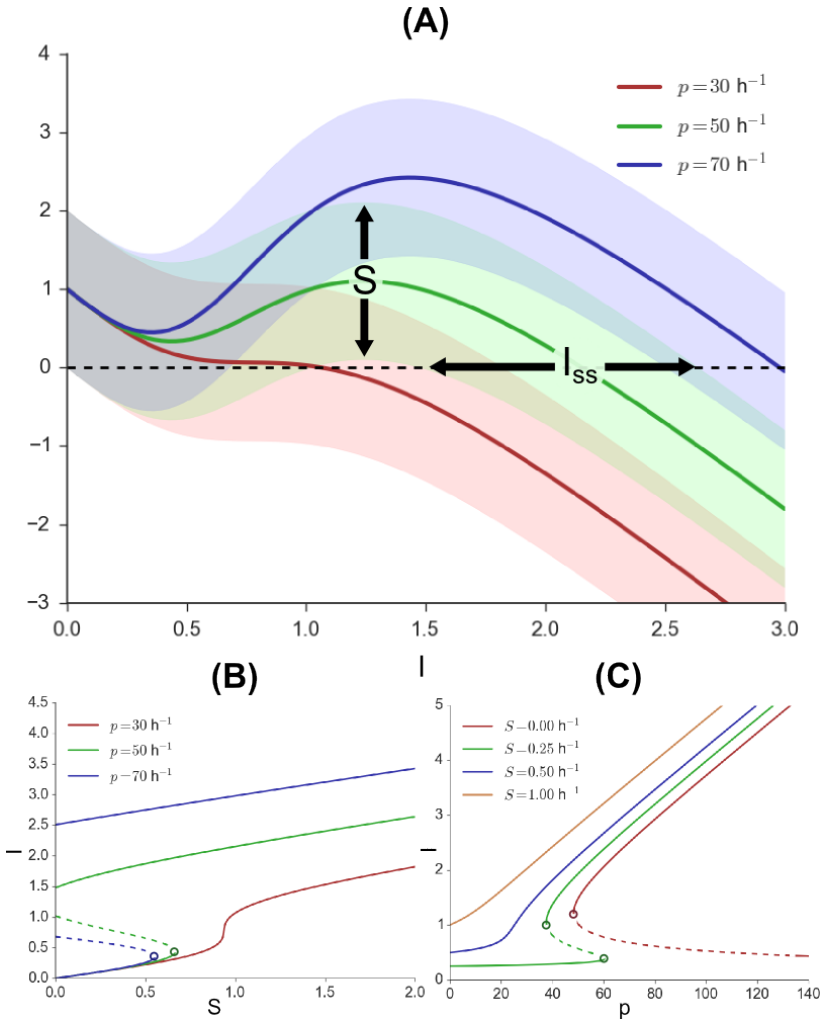

Figure 5.3: Effects of stimuli on steady-state solutions. **(A)** shows the solutions to equation (5.28), for three values of p and $0\ \text{h}^{-1} \leq S \leq 2\ \text{h}^{-1}$. **(B)** and **(C)** are found by rewriting equation (5.27), to have S, and p on the LHS respectively and plotting the solution along the x-axis, and the variable along the y-axis. **(B)** and **(C)** show that when $p < p_c$, if S is as low as $S = 0.25\ \text{h}^{-1}$ we still have a bifurcation point, meaning that S actually lowers the critical p.

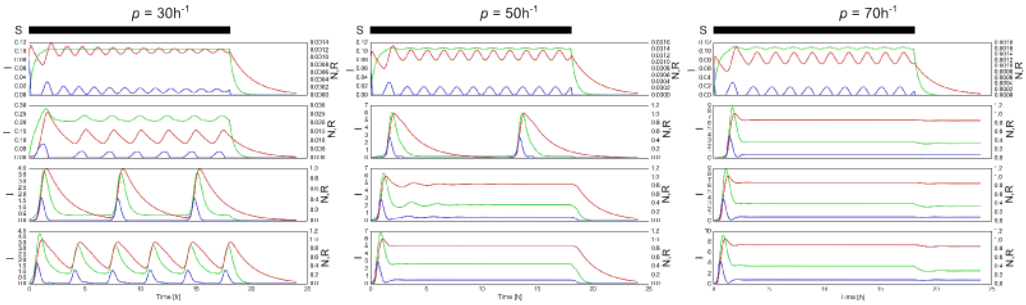

Figure 5.4: Model oscillations, and stabilization as a function of various values of S at three values for p. The top row is for $S = 0.25$ h^{-1}, the second row is for $S = 0.5$ h^{-1}, the third is for $S = 1.0$ h^{-1}, and the last row is for $S = 2.0$ h^{-1}. The source is turned of after $t = 18$ hours, and we see how only a simulations with p much greater than p_c is able to sustain the CIS, while simulations with $p \approx p_c$ can sustain the CIS while the stimuli is on, given that it is high enough, but fails to stay in the inflammatory state when the source term is set to zero. For $p < p_c$ we see how not even $S = 2.0$ h^{-1} is enough for exciting the system into the high steady-state. The reason for this is of course, as is seen in figure 5.3**(B)**, that the only solution to equation (5.28) is the zero point when p is this low.

The general solution to this quartic equation is quite lengthy, but we can plot the LHS as a function I with various values of p and S. In figure 5.3**(A)** three values of p are plotted with $S = 1$ h^{-1}, shown as the solid lines, while the the semi-transparent areas are the plots of p in the range 0 h$^{-1} \leq S \leq 2$ h^{-1}. What we see for $p = 30$ h^{-1} (the red line and area) is that when $S = 0$ h^{-1}, there is no solution except the zero point, which is of course what we expect for $p < p_c$. However, by increasing S, we suddenly find that the steady-state of I increases to a non-zero value. A little more interesting is the case of $p = 50$ h^{-1} (the green line and area), where with $S = 0$ h^{-1} the steady-state has three solutions. By increasing S gradually $S = 1$ h^{-1} (the solid green line), we increase the distance between the high concentration stable fixed point and the unstable fixed point, and decrease the distance between the low concentration fixed point and the unstable fixed point. Then as S reaches a certain value, the zero point and the unstable fixed point merge into one, and increasing S above this value, makes the only solution the high concentration fixed point. This can also be seen in figure 5.3**(B)**. Figure 5.3**(C)** is again a $p - I$ phase-plane plot made to illustrate the effects of S on the bifurcation of I as a function of p. It shows how a small $S = 0.25$ h^{-1} has moved the stable- and unstable fixed node very close, and that an S as low as $S = 1$ h^{-1} entirely removes the bifurcation point and makes the only solution the high concentration steady state. To see the effects of the stimulus we can have a look at figure 5.4, which shows the dynamics of the model for various values of S at three values of p, where one is lower than p_c, one is almost equal to p_c, and the last is greater.

We have now looked at the most important parts of the stationary model, that is still applicable to a motile model. Of course, when taking the diffusion term into consideration as well, there are other factors that play a role, like influx of cytokines from neighboring cells, and loss of cytokines through diffusion. We will not go into this, but interested readers can read [Holst-Hansen, Chp.4 Model Analysis, Appendix A, and Appendix B] for a very nice derivation of an approximate solution to the steady-state of equation (5.3) for an islet of cells. What is worth noting, is that for a group of macrophages in equilibrium, the diffusion term and source term are approximately equivalent. This occurs, because in a group of macrophages, the total irretrievable loss from diffusion becomes lower as the number of macrophages grow. This essentially means that the derivations done in this chapter could effectively be applied to a system of macrophages in equilibrium. In the following chapter, we will take a look at the simulations, and what can be derived from these simulations.

6

Simulation Results and Discussions

"If you're going through hell, keep going"
– Winston Churchill

Throughout the thesis we have developed a sound understanding of how small changes to particular parameters can have an immense effect on the dynamics of a single macrophage. Though these analytical results are interesting, they were developed under various assumptions and conditions that aren't valid when looking at a system of macrophages. Some of these include, the assumption of no diffusion used to find the steady-state solutions to the cytokine partial differential equation and the no source term. These analytical solutions therefore only serve the purpose of illustrating the various states of the macrophage, and how small changes in the system can lead to very different results.

Simulations however, allow us to numerically show how such a system of macrophages behaves under various conditions. Through simulations we can investigate spatial and temporal profiles of a system of macrophages, and seek answers to questions such as, how does macrophage self-regulation occur, how is the average plaque size related to the positive feedback parameter p and the density of the macrophages, and how is a low diffusion constant system different from a high diffusion constant system? These are some of the questions that will be examined in this chapter.

The chapter will start by describing how plaques are defined, and how their size will be measured, as well as some general data analysis used for the results. This will be followed by looking at the effects of low and high cytokine diffusion constants and on average plaque size. Using fixed values of D and S, we will proceed to find answers to questions such as how and when does self-limitation, i.e. localized non-spreading chronic inflammation

occur? And what can be done to resolve plaques? Each simulation setup will be described and the results discussed.

6.1 Plaque Definition and Data Analysis

Before we go into the simulations, how they are done and their results, we will need to define some types of measures, e.g. how can we from a simulation evaluate the average plaque size, and how is average plaque size defined?

Each simulation saves the location of every macrophage, the cytokine levels of the entire grid and the ensemble average of each macrophages NF-κB, inhibitor and cytokine levels. Some of the simulations will save this data for every n'th hour where n is mostly chosen to be $n = 0.1$. Simulations where we are only interested in the configurations at the end, will only save the last data configuration. To extract meaning from the data, I will in many cases look at averages of various values. In the case of plaque size, a single plaque is found through a breadth-first search (BFS) of the data. Defining the location of each macrophage as:

$$\mathbf{x} = [(x_1, y_1), (x_2, y_2), \ldots, (x_{N_{mp}}, y_{N_{mp}})]$$

and the cytokine levels of the entire grid as:

$$\mathbf{C} = \begin{pmatrix} c_{11} & c_{12} & \ldots & c_{1N} \\ c_{21} & c_{22} & \ldots & c_{2N} \\ \vdots & \vdots & \ddots & \vdots \\ c_{N1} & c_{N2} & \ldots & c_{NN} \end{pmatrix}$$

we can define an array consisting of all the macrophage locations where the cytokine levels are significant:

$$\mathbf{x_c} = \{(x, y) | (x, y) \in \mathbf{x} \, : \, \mathbf{C}_{x,y} > 0.05 \mathrm{h}^{-1}\}$$

The choice of 0.05 h^{-1} as the significant level of cytokines was done empirically, based on simulations. The reason it was chosen based on simulations, was that the maximum cytokine levels of the grid depends very highly on the parameter p, the number of macrophages in the grid, and the diffusion constant D. This meant that calculating a maximum cytokine level, would be very problematic, and therefore the choice of a significant cytokine level also became very problematic. Choosing a significant level of 0.05 h^{-1} was therefore done to eliminate macrophages from moving towards very small cytokine gradients, while still allowing them to see small, but not insignificant levels of cytokines, in their environment, giving rise to some

randomness. To find the plaques from this array we can pick a random (x_R, y_R), and do a BFS. If the randomly chosen location is part of the only plaque in the system, then the BFS will return the entire array $\mathbf{x_c}$. If however there are multiple plaques, a BFS on $\mathbf{x_c}$ will return all the locations that can be reached from (x_R, y_R). To find the rest of the plaques one can remove the locations that were reachable from (x_R, y_R) from $\mathbf{x_c}$ and do another BFS. This continuous until $\mathbf{x_c}$ is empty. Now the length of the BFS on $\mathbf{x_c}$ will be the number of macrophages in that plaque. It should be noted that if the BFS returns only less than three macrophages this result will be overlooked. The reason these results are overlooked is that cytokine waves can lead to macrophage locations having a high cytokine levels without the macrophage actually producing cytokines or being part of a plaque. Now because $\Delta x = \Delta y = 1$ the number of macrophages in a plaque is actually equal to its size $A_{plaque} = N_{mp}$. The average plaque size of a simulation is found by averaging the plaque sizes:

$$\mu_A = \frac{1}{n}\sum_{i=1}^{n} A_{plaque,i}$$

and the standard deviation is:

$$\sigma_A = \sqrt{\frac{1}{n}\sum_{i=0}^{n}(A_{plaque,i} - \mu_A)^2}$$

When we are doing more than a single simulation on a specific parameter set, we will want to find the mean over the simulations. Since we are assuming that we are essentially simulating a real world phenomenon, we expect the results to be consistent, given the same initial conditions. But we also know that, because of randomness, introduced by movement of the macrophages, or by the manner of which cells diffuse cytokines, there will be some variations to the simulations. Since the simulations are independent, and because of our assumptions, we can make use of the Central Limit Theorem, which states that taking the sum of K independent variables drawn from a distribution with a mean μ and variance σ^2, the expected value of the sum is equal to the sum of the means[Barlow, 1989]. W.r.t. our simulation it means that the mean of μ_A is a better estimate for the true mean and is given as:

$$\langle A_{plaque} \rangle = \bar{\mu} = \frac{1}{K}\sum_{i=1}^{K} \mu_i$$

where K is the number of simulations, and has the variance:

$$\bar{\sigma^2} = \frac{1}{K}\sum_{i=1}^{K} \sigma_i^2$$

Now that we have a definition of the plaque size and how they are calculated, we can start analysing simulation results.

6.2 Parameter Evaluations

As was stated earlier in the study, cytokine diffusion, D, cytokine stimuli S, and positive feedback on cytokine production p are variables that we either don't have a well defined value for or a free parameter. To alleviate the problem of doing all the simulations for all possible values of D, S, and p, this section will show how these parameters affect the average plaque size. The ultimate goal of these simulations, is to show that a rescaling of the diffusion is equivalent to resizing the grid, meaning we can choose a fixed diffusion constant for the rest of the simulations and focus on the qualitative results, as the quantitative results can be rescaled.

From simulations we wish to find the minumum p for a system of motile macrophages to exhibit sustained inflammation. Furthermore we want to find out if there is a relationship between the average plaque size and the diffusion constant, and the average plaque size and the amount of macrophages in the system.

6.2.1 Minimum p for Sustained Inflammation in a Motile System

To find out how the minimum p is affected by the diffusion constant, a simulation was set up to run for $t = 60$ hours, where the source S was on for the first $t = 24$ hours, with a fixed p and D. This was done to see if any self-sustaining plaques had developed. If the system dropped to the healthy state, i.e. no inflammation, no such plaque had developed and the simulation was stopped and p was increased. The simulations were done for $S \in [22, 222]$ h^{-1} and $D \in [2, 202]$ cells^2/h and each simulation was done four times. However, the simulations were only done for $S + 20 = D$, since a diffusion constant much higher than the source term would result in the defective macrophage not getting excited. Furthermore, since we are more interested in the state of the system when S is turned off, an S higher than D increases the probability of exciting the system into the inflammatory state. The results are plotted in figure 6.1. Figures 6.1**(A)** and 6.1**(B)** show how the minimum p needed for sustained inflammation at a given D increases as well as how the increasing diffusion constant affects the average plaque size. From figure 6.1**(B)** we also see that the average plaque size of a motile excitable medium around the minimum $p \equiv p^*$ depends linearly on the diffusion constant. What we don't see in figure 6.1**(B)**, are the large errorbars for $D = 2$ cells^2/h, which stretch from $\langle A_{plaque} \rangle = 2$

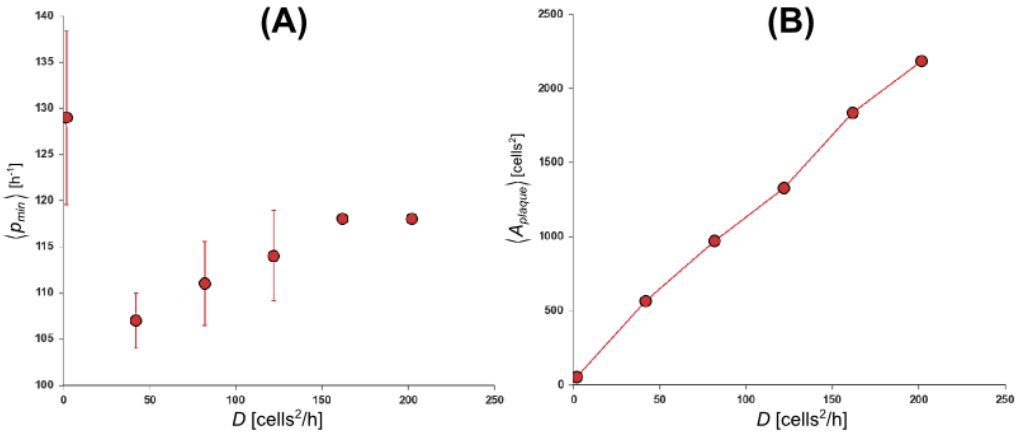

Figure 6.1: These figures show **(A)** how the minimum p is affected by the increasing diffusion constant, and **(B)** how an increasing diffusion constant leads to larger plaques. Because of very small varioations in the results of **(B)**, the errorbars aren't visible. **(B)** very interestingly shows that there is a linear dependence of the plaque size on the diffusion constant.

macrophages to $\langle A_{plaque} \rangle = 35$ macrophages. This uncertainty is also seen in figure 6.1**(A)**, for $D = 2$ cells^2/h, where we see how there is a large uncertainty in the minimum p needed for sustained inflammation. It should be noted, and is visible in figure 6.2, that these simulations led to the system always being locally inflamed, i.e. only a central chronically inflamed plaque around the defect macrophage, except for $D = 2$ cells^2/h. This result actually simplifies the choice of S for the rest of the simulations, since it means that a higher diffusion constant doesn't change the qualitative results, but merely scales them. One reason that there's a larger uncertainty when D is small is that the low diffusion constant means a slow spread of the inflammation resulting in the system not reaching, or very slowly reaching a stable-state. The issue w.r.t. this simulation is that the state of the system at $D = 2$ cells^2/h at $t = 60$ h, is not a stable inflammatory state, but an oscillatory state. Because most MS symptoms develop abruptly within hours or days [Rolak, 2003], a too low diffusion constant, that after $t = 60$ h hasn't reached any form of chronically inflammatory state, can't be used. The choice of diffusion coefficient in the following simulations will therefore be $D = 162$ cells^2/h. This choice lies in the range of possible diffusions values presented in section 3.1.2 and has the lowest standard deviation in minimum p presented in this section. The chosen diffusion constant is also lower than the diffusion constant for IL-1β of $D = 3 \cdot 10^{-7}$ cm^2/s $= 244$ cells^2/h, but slightly higher than the effective diffusion constant of $D_{eff} = 122$ cells^2/h. We can therefore still argue that this is an effective diffusion constant of the cytokines, and most importantly our choice of diffusion constant gives rise to less uncertainty in p^*.

6.2.2 Average Plaque Size

To see how the p parameter affects the plaque size a simulation was set up which uses the previously chosen value of $D = 162$ cells^2/h and runs from $p = 118$ h^{-1} to $p = 718$ h^{-1}, with a macrophage grid density of $\rho = 0.10$ to $\rho = 0.30$. Again S was on for the first $t = 24$ hours, and the simulation ran for $t = 60$ hours. The figure 6.3**(A)** and **(B)** show the results of these simulations. Figure 6.3**(A)** shows how increasing p, for a fixed N_{mp} in almost all cases actually lowered the average plaque size. The interesting part of this result, is that it shows that when p is close to the minimal p needed to excite the system most of the macrophages will accumulate into one large plaque. If however p is higher, less macrophages are needed to sustain and excite the plaques and the macrophages will instead form into many smaller plaques. in figure 6.3**(B)** it is a bit easier to see how increasing p and N_{mp} affects the average plaque size. On this figure we see that increasing the number of macrophages, does not introduce any qualitative changes in the results. In fact, increasing the number of macrophages just scales the plaque size linearly, at least for high p. Close to the critical value there is high variation.

Since there are no qualitative changes in the results found by increasing the number of macrophages there is no reason to run the simulations for other than one value of N_{mp}. However, this will be done for one of the following simulations in which we want to see if plaques can grow infinitely given enough macrophages.

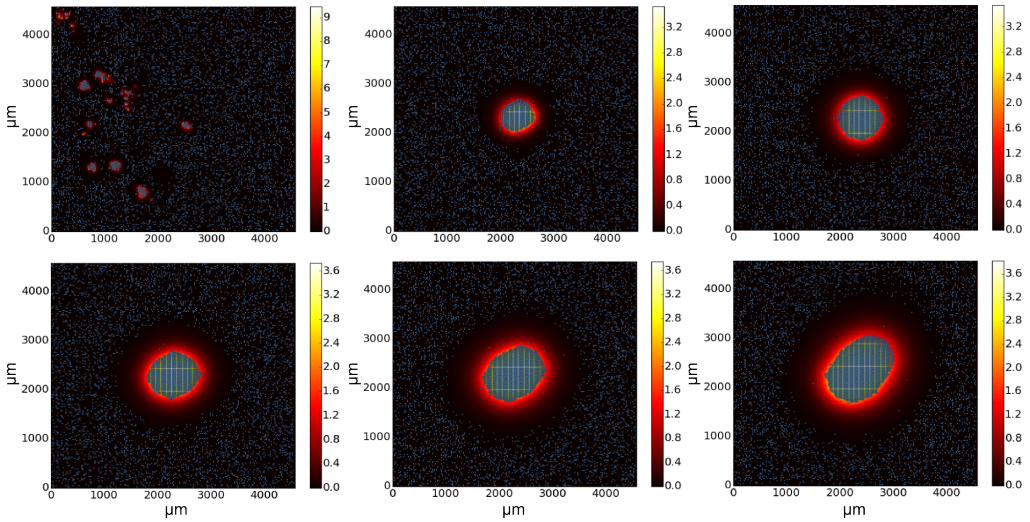

Figure 6.2: Formation of the central plaque for $S \in [22, 222]$ h^{-1} and $D \in [2, 202]$ cells^2/h. Five of the six simulations, show the same qualitative results, except for $D = 2$ cells^2/h and $S = 2$h^{-1}.

To sum up this section, we found that the qualitative results were the same, when increasing diffusion constant and number of macrophages. We could therefore choose a fixed D, and N_{mp} for the rest of the simulations. The choice of $D = 162$ cells^2/h fell on a value slightly higher than the effective diffusion constant reported in [Goodhill, 1997], while the number of macrophages $N_{mp} = 0.15 \cdot N_x N_y$ cells, was chosen from the average macrophage density reported in [Nimmerjahn et al., 2005]. The choice of $S = 182$ h^{-1} was not specified based on any experimental results, but was chosen based on the results of section 6.2.1, and because a S slightly higher than D would ensure a net production of cytokines, making the transition to the inflammatory state more probable.

6.3 Self-Regulation

In the previous section, we saw that when $S = D$ and $p \approx 118\text{h}^{-1}$ the formation of a central plaque, with no other plaques happend for all $D = S \neq 2$. We therefore know that self-regulation is a normal occurence in the model and not a numerical artifact or something that is very unlikely to happen. One of the most important questions this thesis sets out to answer, is under which circumstances macrophages accumulate in self-sustained groups. In other word how does self-regulation of chronic inflammatory states occur, and what are the criteria for such to happen?

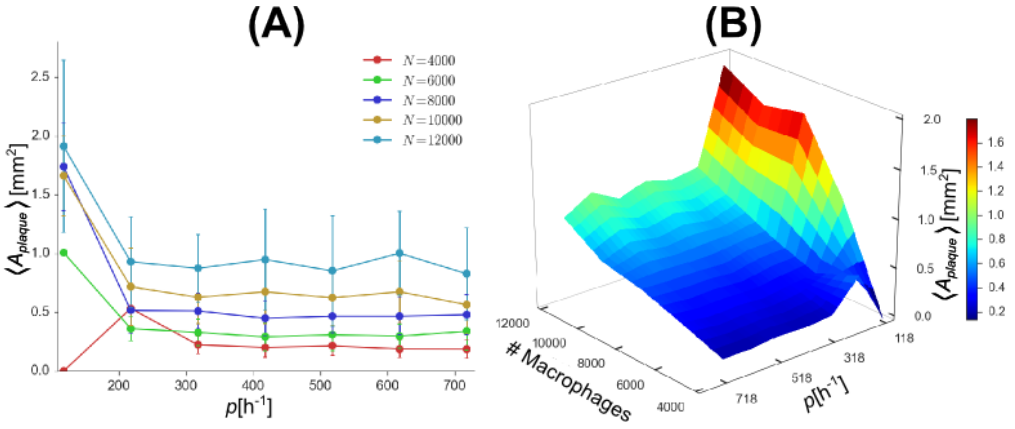

Figure 6.3: Figures showing how the average plaque size is affected by p and N. **(A)** shows change in plaque size as p increases for various values of N_{mp} as well as the standard deviation. **(B)** shows the average plaque size surface, and how both a change in p and N_{mp} affects the average plaque size.

6.3.1 Plaque Development

In most forms of MS, and other demyelinating diseases, plaques are localized states, meaning they don't spread indefinitely. But, given that cytokine waves can be spread over a very large area, given enough proponents, what limits plaques from growing indefinitely, is a question that is worth trying to answer. In the most common form of MS, called RRMS, plaques are randomly distributed and have an average plaque size of 72 ± 21 mm^2 using T2W imaging, and 91 ± 35 mm^2, using FA-maps [Agamanolis; Brownell and Hughes, 1962; Kealey et al., 2005]. What limits their growth is of course a very complex question and whose answer at the current date is incomplete, but as the simulation results will show, given the right range of parameters, it can be explained by the simple fact of a macrophage depleted zone. This process is what in the study is called self-regulation, and it is the process by which, the defective macrophage, only attracts the very nearest neighboring macrophages, creating a central plaque. This attraction of only the nearest macrophages means that a zone free from macrophages will emerge creating a buffer zone between the chronically inflamed central plaque and the rest of the macrophages. If however more macrophages were introduced to the depleted zone, the plaque would increase in size only limited by the size of the grid and the number of macrophages.

To answer these questions, two simulations were set up. The first one to show the accumulation of macrophages in a central plaque which was separated from the rest of the macrophages by a delimited zone. The second one to show that the size limit of the plaque only depends on the amount of available macrophages.

6.3.2 Localized Chronic Inflammation

From sections 6.2.1 and 6.2.2, we saw that a central plaque formed when p was close to $p^* \approx 118$ h^{-1}. To see how such a plaque formed, a simulation was set up to see the temporal evolution of the system. To see the qualitative difference between the formation of one large plaque and many smaller plaques, this simulation was done for various p. The source term was set to $S = 182$ h^{-1}, diffusion constant to $D = 162$ cells^2/h, and positve feedback of cytokines p was $p = 118$ h^{-1}, $p = 168$ h^{-1}, $p = 218$ h^{-1}, and 268 h^{-1} for the four simulations.

The results of the simulations show that the emergence of a central chronically inflamed plaque, is highly dependent on the value of p. For the simulations with $p > p^*$ the inflammation wasn't contained in a central plaque, but spread to the entire system creating many small plaques. More importantly it proves the existence of the localized chronically inflamed plaque, which occurres because of the depleted zone. The temporal

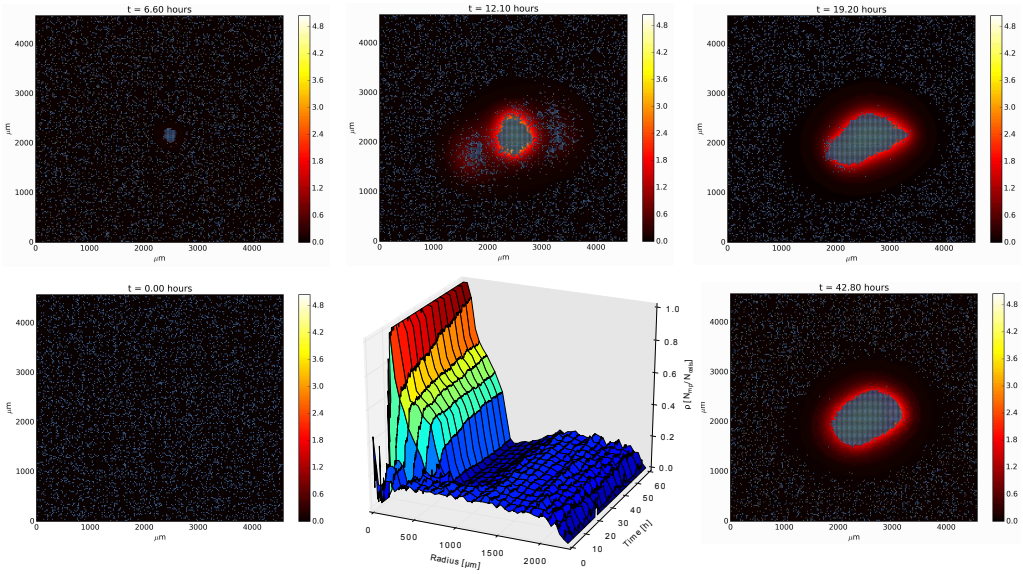

Figure 6.4: Simulations of temporal development of a central plaque, with $p = 118$ h^{-1}. A defective macrophage introduces a production of cytokines into the tissue resulting in a central plaque isolated from the rest of the macrophages by a depleted zone. In the center we see the temporal development of the radial density, and around this we see images of the macrophage movement and cytokine diffusion at various frames.

development seen in the surface plot of figure 6.4 is produced by looking at the radial density. This radial density data is found by taking the sum of all macrophages in the area $A_{radial} = \pi R^2_{outer} - \pi R^2_{inner}$. For this plot the grid was split up into forty radii's. The rest of the simulation results, i.e. $p = 168$ h^{-1}, $p = 218$ h^{-1}, and $p = 268$ h^{-1}, are plotted in figure 6.5, where the temporal development is plotted in the central column, the initial burst of cytokines in the left column, and the chronic inflammatory state in the right column. As for $p = 118$ h^{-1}, all of these simulations start with the formation of a single plaque in the center, but because of the higher p, inflammation is spread to the entire grid. The results from this section showed that the model gives rise to two types of plaque formation. One being the formation of a central chronically inflamed plaque isolated from the rest of the system. The other was the formation of multiple plaques, where most if not all of the macrophages of the system were included. In the most common types of MS, a plaque usually consists of one large scarred area, consistent with a central chronically inflamed plaque, and not a collection of scarred areas. Howeveer this is not the case for more aggressive types of MS, where e.g. Baló's sclerosis produces concentric plaque patterns. Therefore it is fair to consider if a p high enough to create multiple small plaques might be describing the more aggresive MS types, while a low p describes the more common types of MS.

6.3.3 Plaque Size Limit

The simulation starts with $N_{mp} = 400$ macrophages and with a stepsize of 400 macrophages iterates all the way up to $N_{mp} = 6000$ macrophages. The simulation also starts with a positive feedback rate constant of $p = 48$ h^{-1} and with a stepsize of 5 h^{-1} p grows until a sustained plaque formation is found. The defective macrophage in the center of the grid has a source term of $S = 182$ in all the simulations. All the macrophages were positioned inside a circle of radius $R = \sqrt{N_{mp}/\pi}$ cells to ensure that the depleted zone

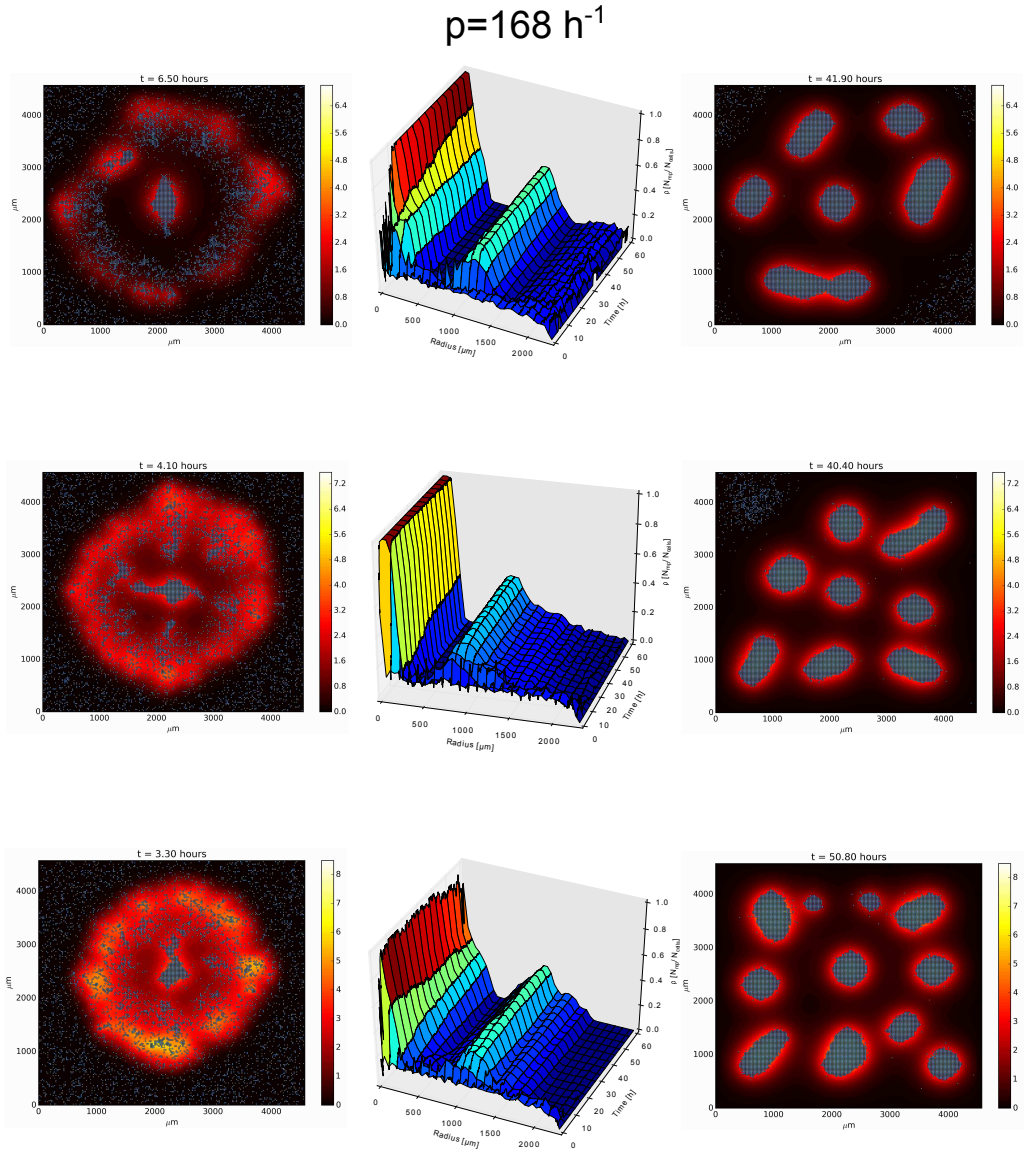

Figure 6.5: Temporal development of systems at various p along with initial cytokine wave and stable chronic plaques.

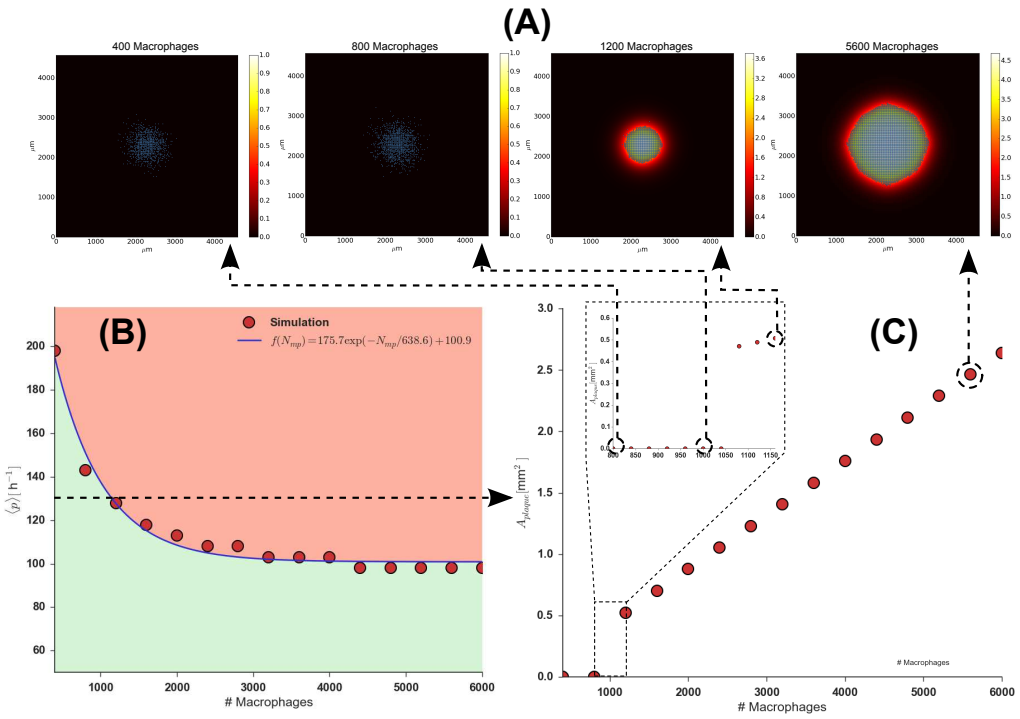

Figure 6.6: Results of plaque size simulations. **(B)** shows the minimum p needed for N_{mp} macrophages to transition to the locked state. The dashed line at $p = 128$ h^{-1} is represented by some data points in **(C)**, where the black dots are the ones that have been illustrated in **(A)**. Furthermore, we see from the figures **(A+C)** that given a fixed p and a growing number of macrophages, the central plaque increases linearly.

didn't emerge. The simulation ran for 60 hours with a stop of the source term at 24 hours. Ensuring that the depleted zone didn't emerge meant that the entire plaque would get inflamed if plaque size was limitless.

Figure 6.6 **(A)** shows the final state of four different simulations, and shows that given a p there exists a critical number of macrophages, needed for a transition into the locked state. Together with figure 6.6**(C)** it also shows that increasing the number of macrophages above a critical value just increases the plaque size, which proves definitively that the plaque size is only bounded by macrophage depletion. This critical number of macrophages is connected with the amount of cytokine produced by the interior macrophages and the amount of cytokine lost by diffusion at the boundary macrophages and by cytokine dilution or degradation. This is also why a larger p means that a lower amount of macrophages are needed to transition into the locked state, which is illustrated in figure 6.6 **(B)**. From this figure we also find that the minimum p needed for locked state transition, decreases towards a critical p, which is found by fitting the data to an exponential decay to be $p_{crit} \approx 100.9$. The asymptotic behaviour

towards the critical p occurs because as the plaque increases in size, the difference between the total production- and total loss of cytokines gets larger. This can be understood by realizing that the area of the plaque increases linearly with the number of macrophages, whilst the circumference of the plaque only increases proportional to the square root of the number of macrophages. Since the production of cytokines depends on the number of macrophages we can define a production term as

$$P \propto N_{mp} p N \tag{6.1}$$

where N is NF-κB. Irretrievable loss of cytokines only occurs for two reasons. The first is the lifetime of the cytokine, and the second is the loss of cytokines at the border of the plaque. The irretrievable loss of cytokines from diffusion, will because of its square root dependence on the number of macrophages have less significance in the total loss as the number of macrophages grows very large. The loss from cytokine dilution or degradation is also proportional to the number of macrophages, and we can therefore define a loss term as

$$L \propto N_{mp} \frac{I}{\tau_I} + \sqrt{N_{mp}} D \nabla^2 I \tag{6.2}$$

Furthermore, we know that a plaque that is chronically inflamed, is actually in a steady-state, meaning $N \to N_{ss}$ and $I \to I_{ss}$, and thus the net change in cytokine levels per timestep should be zero. Putting these two terms together, we end up with an equation that is very similar to the single macrophage equation for $\frac{\partial I}{\partial t}$ from section 5.1.1:

$$\frac{\partial I}{\partial t} \propto P - L = 0 \tag{6.3}$$

$$N_{mp} p N_{ss} = N_{mp} \frac{I_{ss}}{\tau_I} + \sqrt{N_{mp}} D \nabla^2 I_{ss} \tag{6.4}$$

Rewriting it as a function of p, we get:

$$p = \left(\frac{1}{\tau_I} + \frac{D \nabla^2}{\sqrt{N_{mp}}} \right) \frac{I_{ss}}{N_{ss}} \tag{6.5}$$

When N_{mp} becomes very large, we can neglect the diffusion term giving us:

$$p = \frac{I_{ss}}{N_{ss} \tau_I} \tag{6.6}$$

Which is essentially the equation (5.6). This shows that as the plaque size grows, the critical p needed for exciting and sustaining a plaque grows closer to the critical p for a single cell. This behaviour was also observed in

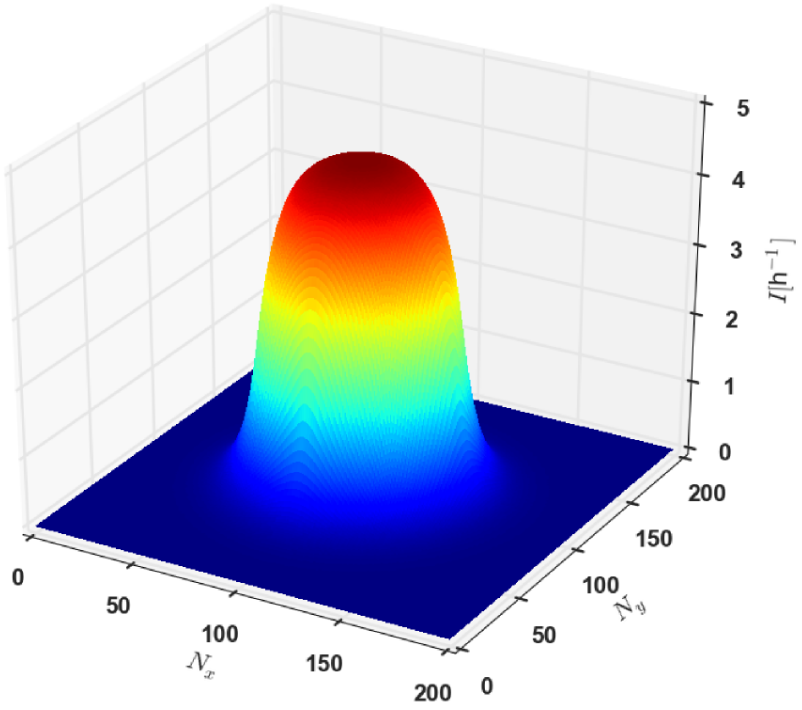

Figure 6.7: The cytokine profile of a plaque of approximately 1900 macrophages.

[Holst-Hansen]. But as we see from the fitting the simulation results to an exponential decay, the critical p from the simulations is almost twice as large as the value found for a single cell and is about 18 h^{-1} lower than the minimal p found in section 6.2.1. The reason the value is almost twice as large as the one found analytically is most likely because the diffusion constant is quite high, and we assumed that the production and loss of cytokines was equal for every macrophage in the plaque. However, as we can see in figure 6.7, the cytokine profile doens't have a sharp boundary, meaning that the production and loss of cytokines isn't the same for each macrophage. This also means that we would need quite a lot more macrophages for the diffusion term to be negligible. The reason that this p is slightly smaller than the value found in section 6.2.1 can be because in this simulation we forced the macrophages to be accumulated. In the other simulation, macrophages were free to move about, and it took a slightly greater p to attract enough macrophages to excite the system.

To sum up this section, we found that self-regulation was precipitated by macrophage depletion. The depletion of macrophages was caused by the central defective macrophage only attracting nearby macrophages. This gave rise to a central plaque seperated from the rest of the macrophages by a depleted zone. We also found out under the assumptions that cy-

tokine production and loss is approximately equal for every macrophage in a plaque, very large plaques effectively behave like a lossless single cell. Furthermore, we found out that the size of the plaque is limited only by the number of macrophages.

6.4 Resolving Plaques

Now we have seen how plaques can form into either one or multiple plaques, which are self-sustaining. In this secion we want to analyse methods to resolve these plaques by changing some of the variables of the system after the onset of chronic inflammation. The simulations in this section will be based on two ways of resolving plaques which were discussed in section 5.1.2. The first will be to lower p and the second to lower k_{IN}.

6.4.1 Lowering Cytokine Through p

The previous section investigated the instigation of plaque formation and plaque self-regulation. Yet we haven't investigated the stability of the plaques which in itself is interesting for the sustainability of plaques and for resolving them. Therefore we will in this section look into what the minimum p needed to sustain an inflamed plaque. This will be done by starting a system in an inflamed state at a fixed p and then lowering p by a factor. If this resolves the plaque, we have found the critical value for resolving plaques and if not a greater reduction in p is introduced.

The simulation was set up so that all the macrophages were located in a single plaque. Since we are interested in how easily plaques are resolved as a function of the free parameter p, each simulation was run for $p \in [100, 200]$ h^{-1}, and ran for $t = 60$ hours. After $t = 36$ hours, the parameter p was lowered by a factor x, where $x \in [0.51, 0.99]$. Each simulation was run four times, and the resulting probability of the plaque not resolving can be seen in figure 6.9. From figure 6.9 we see the results of the simulations. The x-axis is the p parameter, the y-axis is the factor we lower p by after the onset of chronic inflammation, and the z-axis is the probability of staying in the inflammatory state. As is very clear from the figure, resolving plaques through inhibition of p is a very poor method. At the lowest p, which we found in section 6.3.3 to be $p \approx 100$ h^{-1}, p needed to be lowered by at least 9% to resolve the plaque. Increasing p by 100 h^{-1}, meant that not even a reduction of 49%, would resolve the plaque. These results indicate that plaques are very stable to changes in the p parameter, and that it takes a great amount of inhibitor to resolve plaques with this method.

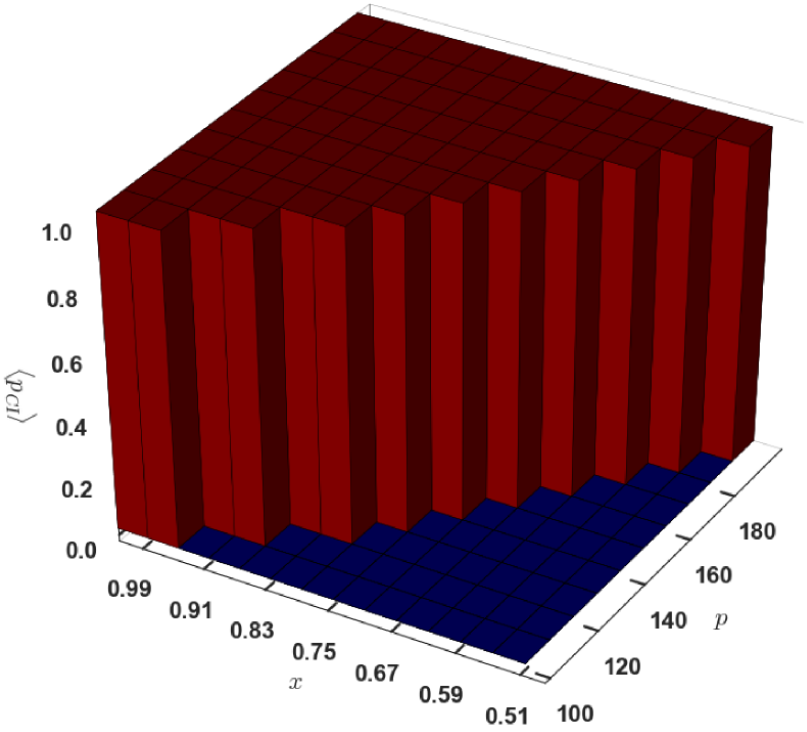

Figure 6.8: Probability of resolving a plaque by lowering p by a factor x after the onset of chronic inflammation. For $p = 100$ h^{-1}, p needed to be lowerd by 9% if the plaque was to be resolved, while a $p = 200$ h^{-1}, couldn't even be resolved by lowering p by 49%, indicating that plaques are very stable to changes in p.

6.4.2 Inhibition of NF-κB Activation

The inhibition of NF-κB activation, was another simulation done to find a method of resolving plaques. As was stated earlier, the study by [Starossom et al., 2012] showed that the inhibition of the NF-κB signaling pathway resulted in resolving plaques. Therefore it would be natural to try to reproduce this behaviour by lowering the NF-κB positive rate constant k_{IN}. The simulation was started with $D = 162$ cells^2/h and $S = 182$ h^{-1}. Because we are still interested in how p affects the lowering of k_{IN}, the simulations were done for $p \in [100, 200]$ h^{-1}. For each value p, k_{IN} was lowered by a factor in the range $x \in [0.51, 0.99]$ and each simulation was done four times. From figure 6.9 we see the results of the simulations. As in section 6.4.1 the x-axis is the p parameter, and the z-axis is the probability of staying in the inflammatory state. In this figure however, the y-axis represents the factor we lower k_{IN} by, and not p. The figure clearly shows how easily a plaque was resolved by lowering k_{IN}. At $p = 100$ h^{-1}, lowering k_{IN} by 13% ensured that the plaque would resolve, while there was a slight uncertainty by only lowering it by 9%. Even increasing p by as much as 100 h^{-1} only

increased the factor we needed to lower k_{IN} by, with 8%. Comparing this with the results of lowering p, this method is slightly worse when p is close to the minimal p, but vastly better when p is greater than the minimal p, indicating that it is a much better method of resolving inflammation than lowering p.

We have in this chapter looked at how plaque formation happens. We started out looking at how the various parameters D, S, p, and N_{mp} affected the plaque size and found that increasing D, S, and N_{mp} didn't change the qualitative results, but merely scaled them. Using this information we looked at how the formation of plaques depended on p, and showed that only around the minimum p needed for excitation of the system into the inflammatory state, would an isolated plaque form in the center. For higher p, the system would settle into chronically inflammatory state with multiple plaques. We then found out that plaques have no size limit, given enough macrophages, and found the minimal p needed to excite a certain amount of macrophages. Last but not least, we looked at methods of resolving inflammation, either by lowering p or by lowering k_{IN}, after the onset of chronic inflammation. This showed that lowering k_{IN} was a much more effective way of resolving plaques than lowering p.

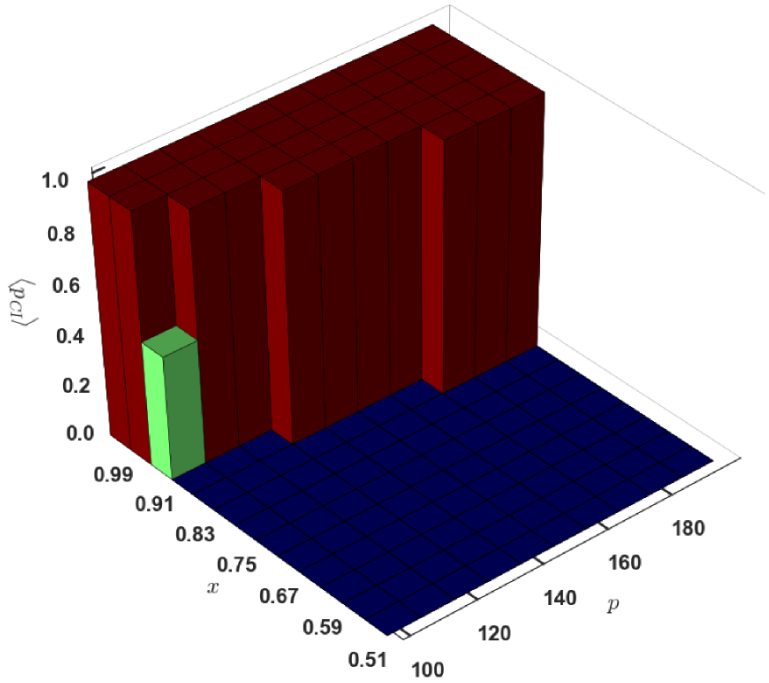

Figure 6.9: This figure shows the probability of plaques staying inflamed, at various values of p, after k_{NI} is lowered by a factor x.

7

Conclusion

"It's more fun to arrive a conclusion than to justify it."
– Malcolm Forbes

Multiple sclerosis is a demyelinating disease of the CNS, that currently affects between 2 and 2.5 million people worldwide[World Health Organization et al., 2008]. The pathogenesis of multiple sclerosis is unknown, but it involves macrophages removing myelin from healthy neurons and oligodendrocytes, resulting in the formation of plaques.

In this study, I used a previously developed model, with the addition of cell motility, to model the inflammatory- and chemotactic process that leads to plaque formation in MS. The inflammation was mediated by the pro-inflammatory cytokines IL-1β, TNF-α, and IFN-γ, which were activated through the NF-κB-complex. Activation of the inflammatory response in macrophages was described by three coupled differential equations and macrophage-macrophage coupling is achieved through cytokine diffusion. The addition of macrophage motility, a novelty in this study, was modeled as a directed random walker, with a cytokine recycling timer $\tau_{Recycle}$, where macrophages moved randomly, when not registering cytokines. However, when registering significant levels of cytokines in one of the eight possible directions in the Moore neighborhood, it would move in this direction for $\tau_{Recycle}$ = 20-30 minutes. The combination of inflammatory response and chemotactic movement means that the model is essentially a three-component motile excitable media. Through a mathematical analyses, it was shown that a single macrophage exhibited three distinct types of behaviour, non-excited, oscillatory, and excited. These behaviours were shown to be highly dependent on the choice of p and S, which were the rate of cytokines production and a basic cytokine production.

Applying the model to a system of macrophages placed on a two dimensional quadratic grid made it possible to simulate the complex processes of inflammation and chemotaxis. Through a parameter evaluation of p, S and D, it was shown that keeping S and D approximately equal, led to the same qualitative results when increasing them. This allowed us to chose fixed values of these for the rest of the simulations. To control system behaviour, the parameter p was free and chosen in the simulations based on the qualitative results.

Multiple sclerosis plaques are in the most common forms of MS of limited size which means something is limiting them. Simulations of lumped macrophages showed that the plaque size could be as large as the number of macrophages. However through simulations of a system of uniformly distributed macrophages for specific values of p, S and D, it was shown that plaque size limit is a naturally occurring phenomenon in the model. The limiting factor being a macrophage depleted zone, creating a gap between the plaque and the rest of the macrophages in the system. The isolating effect of the chemotactic process which results in a chronically inflamed central plaque, actually prevents inflammation from spreading to the rest of the system.

Resolving plaques has been attempted using GAL1, which inhibits the phosphorylation of IκB, thus blocking the production of active NF-κB [Starossom et al., 2012]. Simulations mimicking the experiment showed that lowering the positive feedback from cytokines on NF-κB, effectively resolved plaques when the feedback parameter got low enough. Resolving plaques by lowering p after a chronic inflammatory state had formed, also resulted in resolving the plaques after reaching a critical level, but less effectively than intervening with NF-κB activation.

8

Outlook

Throughout the development of the motile NF-κB model, and its application to the CNS, there have been a number of assumptions and simplifications. These allowed us to analyse a simpler system, than if we had looked at the system as a whole. However, addition of some of the cell types that we discarded could be of great interest, since there are many additional cell types we could implement, giving rise to new exciting interactions and dynamics.

In this last chapter I will describe some of the cells that could be reintroduced to the model as well as what implementing them might result in. Furthermore, I will describe how modifying the NF-κB model could be done and why it could be of interest.

8.1 Oligodendrocytes

The removal of myelin and death of oligodendrocytes leads to non-recovering areas in the brain filled with scars called plaques. In the model, the de- and remyelination phase was disregarded, but introducing them to the model could be an interesting improvement. This was somewhat attempted early on in the study, but wasn't fully developed. Initially simulations showed interesting patterns, but it would need much greater study to conclude anything (see figure 8.1). Implementing oligodendrocytes could be interesting from a modeling point of view, because the removal of oligodendrocytes could act pro-inflammatory, while a complete removal of the oligodendrocytes would result in a non-recovering site. In the current model, if the system gets fixed in a chronically inflamed state, the only way of alleviating this, is to either remove macrophages from the system, or to reduce some of

the parameters, as was shown in section 6.4. If however, oligodendrocytes were a part of the model, de- and remyelination could be analysed.

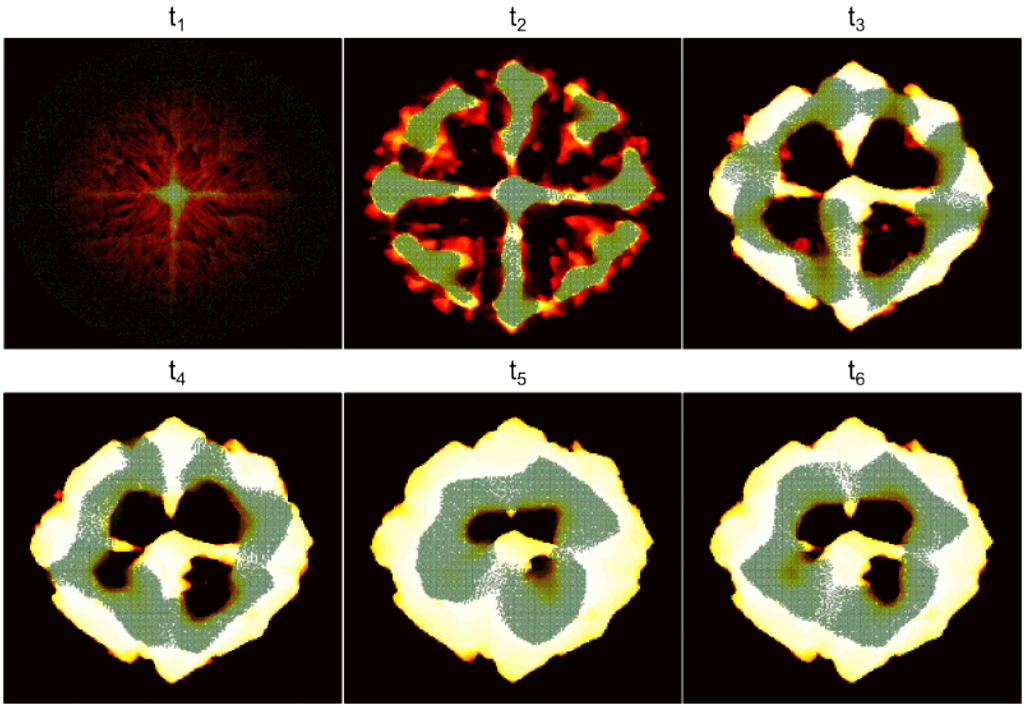

Figure 8.1: Model with additional oligodendrocytes added to the grid. The whiter the area the more dead oligodendrocytes. The six images are frames of a movie with the upper left corner is $t = 1$ hour after simulations start, and the lower right corner is $t = 25$ hours after simulation start.

8.2 M2 Macrophages

The study by [Vereyken et al., 2011] showed that M2 macrophages actually moved faster towards a pro-inflammatory signal than M1 macrophages. The anti-inflammatory reactions of the M2 macrophages, are required for a demyelinated area to recover. Introducing M2 macrophages to the system, with their own anti-inflammatory cytokines, which promote their own proliferation and inhibit M1 differentiation, could introduce some very interesting dynamics. This might affect the size of the plaques. This might limit their growth by enclosing pro-inflammatory macrophages, effectively inhibiting the inflammatory response from spreading to the rest of the system. It might also make the plaques larger, as a plaque consisting of 10% (just a random number) M2 macrophages would require more M1 macrophages to sustain a chronic inflammation.

8.3 Phenotype Switch

The study by [Boven et al., 2006] showed that myelin-laden macrophages, called foam-cells — pro-inflammatory macrophages who have ingested large amounts of myelin — become anti-inflammatory. Implementing this in the model would require the implementation of myelin to the system as well as a myelin ingestion rate and degradation rate. This could be implemented in the same manner as the receptor movement model, where macrophages can ingest 1 unit of myelin, after which it needs τ_{Devour} time to degrade the myelin. This could be implemented on its own or in combination with the addition of oligodendrocytes.

8.4 Arginine

Macrophages require the uptake of the exogenous amino acid arginine to satisfy its metabolic demands. Depending on the intracellular availability of this amino acid it is essential for the macrophages' synthesis of proteins and production nitric oxides[Comalada et al., 2012]. The addition of arginine could be implemented in the model as a resource for cytokine production, effectively limiting this production. Therefore including extra- and intracellular arginine to the model and making cytokine production a function of intracellular arginine, could be very interesting.

Bibliography

Agamanolis, Dimitri P. Demyelinating Diseases. `http://neuropathology-web.org/chapter6/chapter6aMs.html`. Accessed: 07-01-2015.

Ando, Mitsuru; Takahashi, Yuki; Yamashita, Takuma; Fujimoto, Mai; Nishikawa, Makiya; Watanabe, Yoshihiko, and Takakura, Yoshinobu. Prevention of adverse events of interferon γ gene therapy by gene delivery of interferon γ-heparin-binding domain fusion protein in mice. *Molecular Therapy—Methods & Clinical Development*, 1, 2014.

Azevedo, Frederico AC; Carvalho, Ludmila RB; Grinberg, Lea T; Farfel, José Marcelo; Ferretti, Renata EL; Leite, Renata EP; Lent, Roberto; Herculano-Houzel, Suzana, and others, . Equal numbers of neuronal and nonneuronal cells make the human brain an isometrically scaled-up primate brain. *Journal of Comparative Neurology*, 513(5): 532–541, 2009.

Barlow, Roger J. *Statistics: a guide to the use of statistical methods in the physical sciences*, volume 29. John Wiley & Sons, 1989.

Bauer, Jan; Huitinga, Inge; Zhao, Weiguo; Lassmann, Hans; Hickey, William F, and Dijkstra, Christine D. The role of macrophages, perivascular cells, and microglial cells in the pathogenesis of experimental autoimmune encephalomyelitis. *Glia*, 15(4): 437–446, 1995.

Bendtsen, Kristian Moss; Jensen, Martin Borch; May, Alfred; Rasmussen, Lene Juel; Trusina, Ala; Bohr, Vilhelm A, and Jensen, Mogens H. Dynamics of the dna repair proteins wrn and blm in the nucleoplasm and nucleoli. *European Biophysics Journal*, 43(10-11):509–516, 2014.

Biswas, Subhra K and Mantovani, Alberto. Macrophage plasticity and interaction with lymphocyte subsets: cancer as a paradigm. *Nature immunology*, 11(10):889–896, 2010.

Boocock, CA; Jones, GE; Stanley, ER, and Pollard, JW. Colony-stimulating factor-1 induces rapid behavioural responses in the mouse macrophage cell line, bac1. 2f5. *Journal of cell science*, 93(3):447–456, 1989.

Boston University Biology, . NF-κB diseases, 2014.

Boven, Leonie A; Van Meurs, Marjan; Van Zwam, Marloes; Wierenga-Wolf, Annet; Hintzen, Rogier Q; Boot, Rolf G; Aerts, Johannes M; Amor, Sandra; Nieuwenhuis, Edward E, and Laman, Jon D. Myelin-laden macrophages are anti-inflammatory, consistent with foam cells in multiple sclerosis. *Brain*, 129(2):517–526, 2006.

Brogden, Kim A and Guthmiller, Janet M. *Polymicrobial diseases*, volume 11. ASM Press Washington DC:, 2002.

Brownell, Betty and Hughes, J Trevor. The distribution of plaques in the cerebrum in multiple sclerosis. *Journal of neurology, neurosurgery, and psychiatry*, 25(4):315, 1962.

Burt, R. K.; Balabanov, R.; Han, X.; Sharrack, B.; Morgan, A.; Quigley, K.; Yaung, K.; Helenowski, I. B.; Jovanovic, B.; Spahovic, D.; Arnautovic, I.; Lee, D. C.; Benefield, B. C.; Futterer, S.; Oliveira, M. C., and Burman, J. Association of nonmyeloablative hematopoietic stem cell transplantation with neurological disability in patients with relapsing-remitting multiple sclerosis. *JAMA*, 313(3):275–284, Jan 2015.

Cheong, Raymond; Bergmann, Adriel; Werner, Shannon L; Regal, Joshua; Hoffmann, Alexander, and Levchenko, Andre. Transient iκb kinase activity mediates temporal nf-κb dynamics in response to a wide range of tumor necrosis factor-α doses. *Journal of Biological Chemistry*, 281(5):2945–2950, 2006.

Comalada, Mònica; Yeramian, Andree; Modolell, Manuel; Lloberas, Jorge, and Celada, Antonio. Arginine and macrophage activation. In *Leucocytes*, pages 223–235. Springer, 2012.

Compston, Alastair and Coles, Alasdair. Multiple sclerosis. *The Lancet*, 372 (9648):1502 – 1517, 2008. ISSN 0140-6736. doi:http://dx.doi.org/10.1016/S0140-6736(08)61620-7. URL `http://www.sciencedirect.com/science/article/pii/S0140673608616207`.

Dimitri P. Agamanolis, . Multiple Sclerosis and Variante, 2014.

Epstein, Franklin H; Barnes, Peter J, and Karin, Michael. Nuclear factor-κB—a pivotal transcription factor in chronic inflammatory diseases. *New England Journal of Medicine*, 336(15):1066–1071, 1997.

Geiger, Jeremy; Wessels, Deborah, and Soll, David R. Human polymorphonuclear leukocytes respond to waves of chemoattractant, like dictyostelium. *Cell motility and the cytoskeleton*, 56(1):27–44, 2003.

Gilden, Donald H; Mahalingam, Ravi; Cohrs, Randall J, and Tyler, Kenneth L. Herpesvirus infections of the nervous system. *Nature Clinical Practice Neurology*, 3(2): 82–94, 2007.

Ginhoux, Florent; Greter, Melanie; Leboeuf, Marylene; Nandi, Sayan; See, Peter; Gokhan, Solen; Mehler, Mark F; Conway, Simon J; Ng, Lai Guan; Stanley, E Richard, and others, . Fate mapping analysis reveals that adult microglia derive from primitive macrophages. *Science*, 330(6005):841–845, 2010.

Goodhill, Geoffrey J. Diffusion in axon guidance. *European Journal of Neuroscience*, 9 (7):1414–1421, 1997.

Grabher, Clemens; Cliffe, Adam; Miura, Kota; Hayflick, Joel; Pepperkok, Rainer; Rørth, Pernille, and Wittbrodt, Joachim. Birth and life of tissue macrophages and their migration in embryogenesis and inflammation in medaka. *Journal of leukocyte biology*, 81(1):263–271, 2007.

Groves, DT and Jiang, Y. Chemokines, a family of chemotactic cytokines. *Critical Reviews in Oral Biology & Medicine*, 6(2):109–118, 1995.

Herculano-Houzel, Suzana. The human brain in numbers: a linearly scaled-up primate brain. *Frontiers in human neuroscience*, 3, 2009.

Holst-Hansen, Thomas. The inflammatory response in islets of langerhans - Transitions between healthy and destructive behaviour of regulatory network. Master thesis, University of Copenhagen.

Janeway, Charles A; Travers, Paul; Walport, Mark; Shlomchik, Mark J, and others, . Macrophage activation by armed cd4 th1 cells. 2001.

Jensen, Mogens H and Krishna, Sandeep. Inducing phase-locking and chaos in cellular oscillators by modulating the driving stimuli. *FEBS letters*, 586(11):1664–1668, 2012.

Jones, Gareth E. Cellular signaling in macrophage migration and chemotaxis. *Journal of leukocyte biology*, 68(5):593–602, 2000.

Kealey, Susan M; Kim, YoungJoo; Whiting, Wythe L; Madden, David J, and Provenzale, James M. Determination of multiple sclerosis plaque size with diffusion-tensor mr imaging: Comparison study with healthy volunteers 1. *Radiology*, 236(2):615–620, 2005.

Khonsari, Roman H and Calvez, Vincent. The origins of concentric demyelination: self-organization in the human brain. *PloS one*, 2(1):e150, 2007.

Kierdorf, Katrin; Erny, Daniel; Goldmann, Tobias; Sander, Victor; Schulz, Christian; Perdiguero, Elisa Gomez; Wieghofer, Peter; Heinrich, Annette; Riemke, Pia; Hölscher, Christoph, and others, . Microglia emerge from erythromyeloid precursors via pu. 1-and irf8-dependent pathways. *Nature neuroscience*, 16(3):273–280, 2013.

Krombach, Fritz; Münzing, Silvia; Allmeling, Anne-Marie; Gerlach, J Tilman; Behr, Jürgen, and Dörger, Martina. Cell size of alveolar macrophages: an interspecies comparison. *Environmental health perspectives*, 105(Suppl 5):1261, 1997.

Kudo, Shoji; Mizuno, Keiko; Hirai, Yoshikatsu, and Shimizu, Takefumi. Clearance and tissue distribution of recombinant human interleukin 1β in rats. *Cancer research*, 50 (18):5751–5755, 1990.

Li, H; Cuzner, ML, and Newcombe, J. Microglia-derived macrophages in early multiple sclerosis plaques. *Neuropathology and applied neurobiology*, 22(3):207–215, 1996.

Li, Wei and Stanley, E Richard. Role of dimerization and modification of the csf-1 receptor in its activation and internalization during the csf-1 response. *The EMBO journal*, 10(2):277, 1991.

Lublin, Fred D; Reingold, Stephen C, and others, . Defining the clinical course of multiple sclerosis results of an international survey. *Neurology*, 46(4):907–911, 1996.

Martin, Roland; McFarland, Henry F, and McFarlin, Dale E. Immunological aspects of demyelinating diseases. *Annual review of immunology*, 10(1):153–187, 1992.

Martinez, Fernando O and Gordon, Siamon. The m1 and m2 paradigm of macrophage activation: time for reassessment. *F1000prime reports*, 6, 2014.

Martinez, Fernando O; Helming, Laura, and Gordon, Siamon. Alternative activation of macrophages: an immunologic functional perspective. *Annual review of immunology*, 27:451–483, 2009.

Merrill, Jean E and Zimmerman, Robert P. Natural and induced cytotoxicity of oligodendrocytes by microglia is inhibitable by tgfβ. *Glia*, 4(3):327–331, 1991.

Michelsen, Alexandra. Two variable model of inflammatory response - Towards an analytical approach to an excitable media model of propagating cytokine waves. Bachelor thesis, University of Copenhagen.

Minagar, Alireza and Alexander, J Steven. Blood-brain barrier disruption in multiple sclerosis. *Multiple sclerosis*, 9(6):540–549, 2003.

Mohan, TR Krishna; Sen, Surajit, and Ramanathan, Murali. A computational model for lesion dynamics in multiple sclerosis of the brain. *International Journal of Modern Physics E*, 17(05):930–939, 2008.

Nash, Richard A; Hutton, George J; Racke, Michael K; Popat, Uday; Devine, Steven M; Griffith, Linda M; Muraro, Paolo A; Openshaw, Harry; Sayre, Peter H; Stüve, Olaf, and others, . High-dose immunosuppressive therapy and autologous hematopoietic cell transplantation for relapsing-remitting multiple sclerosis (halt-ms): a 3-year interim report. *JAMA Neurol*, 2014.

Nimmerjahn, Axel; Kirchhoff, Frank, and Helmchen, Fritjof. Resting microglial cells are highly dynamic surveillants of brain parenchyma in vivo. *Science*, 308(5726):1314–1318, 2005.

O'Connor, Paul; Wolinsky, Jerry S; Confavreux, Christian; Comi, Giancarlo; Kappos, Ludwig; Olsson, Tomas P; Benzerdjeb, Hadj; Truffinet, Philippe; Wang, Lin; Miller, Aaron, and others, . Randomized trial of oral teriflunomide for relapsing multiple sclerosis. *New England Journal of Medicine*, 365(14):1293–1303, 2011.

Pahl, Heike L. Activators and target genes of Rel/NF-κB transcription factors. *Oncogene*, 18(49):6853–6866, 1999.

Peterson, John W; Bö, Lars; Mörk, Sverre; Chang, Ansi; Ransohoff, Richard M, and Trapp, Bruce D. Vcam-1-positive microglia target oligodendrocytes at the border of multiple sclerosis lesions. *Journal of Neuropathology & Experimental Neurology*, 61 (6):539–546, 2002.

Pixley, Fiona J. Macrophage migration and its regulation by csf-1. *International journal of cell biology*, 2012, 2012.

Poser, CM and Brinar, VV. Disseminated encephalomyelitis and multiple sclerosis: two different diseases–a critical review. *Acta Neurologica Scandinavica*, 116(4):201–206, 2007.

Rapalino, O; Lazarov-Spiegler, O; Agranov, E; Velan, GJ; Yoles, E; Fraidakis, M; Solomon, A; Gepstein, R; Katz, A; Belkin, M, and others, . Implantation of stimulated homologous macrophages results in partial recovery of paraplegic rats. *Nature medicine*, 4(7):814–821, 1998.

Rawji, Khalil S and Yong, V Wee. The benefits and detriments of macrophages/microglia in models of multiple sclerosis. *Clinical and Developmental Immunology*, 2013, 2013.

Reynolds, Ashley; Laurie, Chad; Lee Mosley, R, and Gendelman, Howard E. Oxidative stress and the pathogenesis of neurodegenerative disorders. *International review of neurobiology*, 82:297–325, 2007.

Rolak, Loren A. Multiple sclerosis: it's not the disease you thought it was. *Clinical medicine & research*, 1(1):57–60, 2003.

Ruuls, Sigrid R and Sedgwick, Jonathon D. Cytokine-directed therapies in multiple sclerosis and experimental autoimmune encephalomyelitis. *Immunology and cell biology*, 76(1):65–73, 1998.

Satoh, Jun-ichi; Illes, Zsolt; Peterfalvi, Agnes; Tabunoki, Hiroko; Rozsa, Csilla, and Yamamura, Takashi. Aberrant transcriptional regulatory network in T cells of multiple sclerosis. *Neuroscience letters*, 422(1):30–33, 2007.

Shijie, Jin; Takeuchi, Hideyuki; Yawata, Izumi; Harada, Yohei; Sonobe, Yoshifumi; Doi, Yukiko; Liang, Jianfeng; Hua, Li; Yasuoka, Satoko; Zhou, Yan, and others, . Blockade of glutamate release from microglia attenuates experimental autoimmune encephalomyelitis in mice. *The Tohoku journal of experimental medicine*, 217(2):87–92, 2009.

Skripuletz, Thomas; Hackstette, Diane; Bauer, Katharina; Gudi, Viktoria; Pul, Refik; Voss, Elke; Berger, Katharina; Kipp, Markus; Baumgärtner, Wolfgang, and Stangel, Martin. Astrocytes regulate myelin clearance through recruitment of microglia during cuprizone-induced demyelination. *Brain*, 136(1):147–167, 2013.

Starossom, Sarah C; Mascanfroni, Ivan D; Imitola, Jaime; Cao, Li; Raddassi, Khadir; Hernandez, Silvia F; Bassil, Ribal; Croci, Diego O; Cerliani, Juan P; Delacour, Delphine, and others, . Galectin-1 deactivates classically activated microglia and protects from inflammation-induced neurodegeneration. *Immunity*, 37(2):249–263, 2012.

Stein, Michael; Keshav, Satish; Harris, Neil, and Gordon, Siamon. Interleukin 4 potently enhances murine macrophage mannose receptor activity: a marker of alternative immunologic macrophage activation. *The Journal of experimental medicine*, 176(1): 287–292, 1992.

Strogatz, Steven H. *Nonlinear dynamics and chaos: with applications to physics, biology, chemistry, and engineering*. Westview press, 2014.

Summers, Charlotte; Rankin, Sara M; Condliffe, Alison M; Singh, Nanak; Peters, A Michael, and Chilvers, Edwin R. Neutrophil kinetics in health and disease. *Trends in immunology*, 31(8):318–324, 2010.

Takeuchi, Hideyuki; Mizuno, Tetsuya; Zhang, Guiqin; Wang, Jinyan; Kawanokuchi, Jun; Kuno, Reiko, and Suzumura, Akio. Neuritic beading induced by activated microglia is an early feature of neuronal dysfunction toward neuronal death by inhibition of mitochondrial respiration and axonal transport. *Journal of Biological Chemistry*, 280 (11):10444–10454, 2005.

Vereyken, EJ; Heijnen, PD; Baron, Wia; de Vries, EH; Dijkstra, Christine D; Teunissen, Charlotte E, and others, . Classically and alternatively activated bone marrow derived macrophages differ in cytoskeletal functions and migration towards specific cns cell types. *J Neuroinflammation*, 8:58, 2011.

Vicker, MICHAEL G; Lackie, JOHN M, and Schill, WALTER. Neutrophil leucocyte chemotaxis is not induced by a spatial gradient of chemoattractant. *Journal of cell science*, 84(1):263–280, 1986.

Vogel, DY; Vereyken, EJ; Glim, Judith E; Heijnen, PD; Moeton, Martina; van der Valk, Paul; Amor, Sandra; Teunissen, Charlotte E; van Horssen, Jack, and Dijkstra, Christine D. Macrophages in inflammatory multiple sclerosis lesions have an intermediate activation status. *J Neuroinflammation*, 10:35, 2013.

Walczak, Agata; Siger, Malgorzata; Ciach, Agnieszka; Szczepanik, Marian, and Selmaj, Krzysztof. Transdermal application of myelin peptides in multiple sclerosis treatment. *JAMA neurology*, 70(9):1105–1109, 2013.

Webb, Sarah E; Pollard, Jeffrey W, and Jones, Gareth E. Direct observation and quantification of macrophage chemoattraction to the growth factor csf-1. *Journal of Cell Science*, 109(4):793–803, 1996.

Weischenfeldt, Joachim and Porse, Bo. Bone marrow-derived macrophages (bmm): isolation and applications. *Cold Spring Harbor Protocols*, 2008(12):pdb–prot5080, 2008.

Wingerchuk, Dean M and Lucchinetti, Claudia F. Comparative immunopathogenesis of acute disseminated encephalomyelitis, neuromyelitis optica, and multiple sclerosis. *Current opinion in neurology*, 20(3):343–350, 2007.

World Health Organization, and others, . Atlas: multiple sclerosis resources in the world 2008, 2008.

Yde, Pernille; Jensen, Mogens Høgh, and Trusina, Ala. Analyzing inflammatory response as excitable media. *Physical Review E*, 84(5):051913, 2011a.

Yde, Pernille; Mengel, Benedicte; Jensen, Mogens H; Krishna, Sandeep, and Trusina, Ala. Modeling the NF-κB mediated inflammatory response predicts cytokine waves in tissue. *BMC systems biology*, 5(1):115, 2011b.

A

Code

On the bottom of this page, you'll find an attached CD, with code. The simulations of the model is written in C++, and running it will produce data in the form of text files, which will be zipped into a folder, collecting the data. To generate movies of the simulation, and to do data analyses on the simulation results, Python scripts were written. For convenience, the CD will include a folder in which the most interesting simulations were made into movies. For those of you reading this in a digital format, the code is publicly available on my ***Dropbox***.